

Towards improved drug action: target binding kinetics and functional efficacy at the mGlu2 receptor

Doornbos, M.L.J.

Citation

Doornbos, M. L. J. (2018, September 12). *Towards improved drug action : target binding kinetics and functional efficacy at the mGlu2 receptor*. Retrieved from https://hdl.handle.net/1887/65384

Version: Not Applicable (or Unknown)

License: License agreement concerning inclusion of doctoral thesis in the

Institutional Repository of the University of Leiden

Downloaded from: https://hdl.handle.net/1887/65384

Note: To cite this publication please use the final published version (if applicable).

Cover Page



Universiteit Leiden



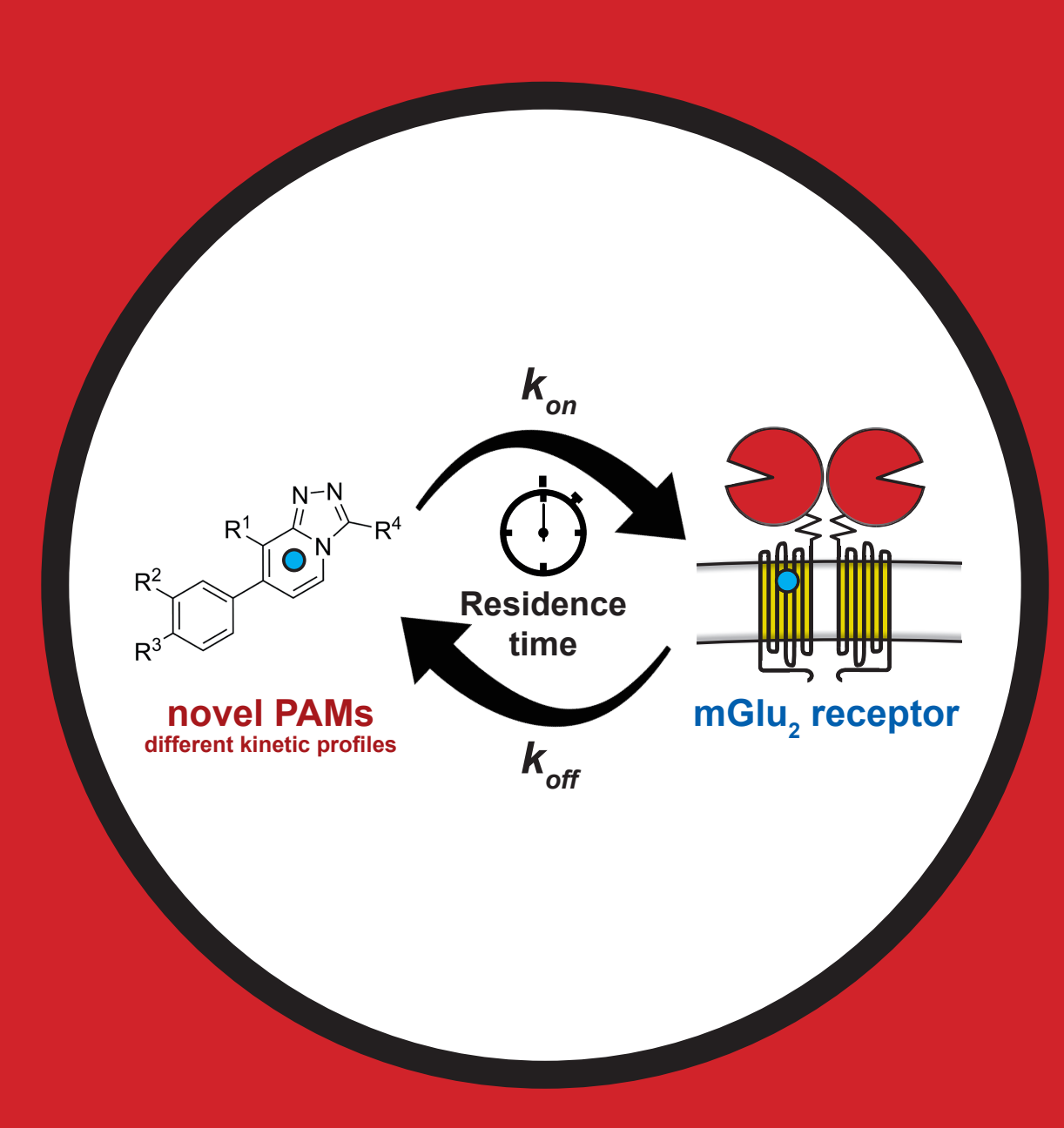
The handle http://hdl.handle.net/1887/65384 holds various files of this Leiden University dissertation.

Author: Doornbos, M.L.J.

Title: Towards improved drug action: target binding kinetics and functional efficacy at

the mGlu2 receptor Issue Date: 2018-09-12





CHAPTER 4

Discovery and kinetic profiling of 7-aryl-1,2,4-triazolo[4,3-a]pyridines: positive allosteric modulators of the metabotropic glutamate receptor 2.

Maarten L J Doornbos, José María Cid, Jordi Haubrich, Alexandro Nunes, Jasper W van de Sande, Sophie C Vermond, Thea Mulder-Krieger, Andrés A Trabanco, Abdellah Ahnaou, Wilhelmus H Drinkenburg, Hilde Lavreysen, Laura H Heitman, Adriaan P IJzerman & Gary Tresadern

Journal of Medicinal Chemistry 60 (2017) 6704–6720. doi:10.1021/acs.jmedchem.7b00669.





ABSTRACT

We report the synthesis and biological evaluation of a series of 7-aryl-1,2,4-triazolo[4,3-a] pyridines with mGlu₂ positive allosteric modulator (PAM) activity and affinity. Besides traditional *in vitro* parameters of potency and affinity, kinetic parameters k_{ont} , k_{off} and residence time (RT) were determined. The PAMs showed various kinetic profiles; k_{on} values ranged over two orders of magnitude, whereas RT values were within a 10-fold range. Association rate constant k_{on} was linearly correlated to affinity. Evaluation of a short, medium and long RT compound in a label-free assay indicated a correlation between RT and functional effect. The effects of long RT compound 9 on sleep-wake states indicated long RT was translated into sustained inhibition of rapid eye movement (REM) *in vivo*. These results show that affinity-only driven selection would have resulted in mGlu₂ PAMs with high values for k_{ont} but not necessarily optimized RT, which is key to predict optimal efficacy *in vivo*.

INTRODUCTION

Glutamate is an important neurotransmitter in the human central nervous system (CNS), where it modulates synaptic responses by activating ionotropic glutamate receptors (iGlu) and metabotropic glutamate receptors (mGlu).1 The eight known mGlu receptors, which belong to the class C G protein-coupled receptors (GPCRs), have been divided into three subclasses based on sequence homology, signaling pathway and pharmacological profile: group I (mGlu_{1.5}), group II (mGlu_{2.3}) and group III (mGlu_{4.6.7.8}).² Structurally, class C GPCRs consist of a large extracellular orthosteric binding domain, the so-called venus flytrap (VFT), a cysteine-rich domain connecting the VFT to the seven-transmembrane (7TM) domain.²³ Group II mGlu receptors are coupled to the $G\alpha_{i_0}$ protein and are generally expressed presynaptically in the periphery of the synapse where they inhibit the release of glutamate upon activation.⁴ The activation of mGlu, receptors has been shown to be a potential strategy for the treatment of psychiatric diseases involving abnormal glutamatergic neurotransmission, such as schizophrenia and anxiety disorder.^{5,6} Drug discovery efforts include the development of positive allosteric modulators (PAMs) for which subtype-selectivity can be more easily obtained as they bind within the less conserved 7TM domain and have little or no intrinsic activity on their own.^{7,8} The mGlu, PAMs N-(4-(2-Methoxyphenoxy)phenyl)-N-(2,2,2-trifluoroethylsulfonyl) pyrid-3-ylmethylamine (1, LY487379)9, Biphenyl-indanone A (2, BINA)10, N-(4-((2-(Trifluoromethyl)-3-Hydroxy-4-(Isobutyryl)phenoxy)methyl)benzyl)-1-Methyl-1H-Imidazole-4-Carboxamide (3, THIIC, also known as LY2607540)11 and 3-cyano-1-cyclopropylmethyl-4-(4-phenyl-piperidin-1-yl)-pyridine-2(1H)-one (4, JNJ-40068782)12 have been characterized both in vitro and in vivo. To date, two mGlu, PAMs have reached clinical trials. The development of 7-methyl-5-[3-(piperazin-1-ylmethyl)-1,2,4-oxadiazol-5-yl]-2-[[4-(trifluoromethoxy)phenyl] methyl]-3H-isoindol-1-one (5, AZD8529) by AstraZeneca was discontinued after a phase 2 schizophrenia trial in which it did not show clinical efficacy when tested as monotherapy. 13,14 Compound 5 recently finished a phase II clinical trial to study smoking cessation in female smokers.15

Meanwhile, the Janssen/Addex mGlu₂ PAM 1-butyl-3-chloro-4-(4-phenyl-1-piperidinyl)-(1*H*)-pyridone (6, JNJ-40411813/ADX71149) met the primary objectives of safety and tolerability in an exploratory phase IIa study in schizophrenia. Moreover, patients treated with antipsychotics who experience residual negative symptoms were identified as the subgroup that may potentially benefit from add-on treatment with 6, although this is yet to be established in a formal proof-of-concept study. In addition, in a second phase IIa study with 6 as adjunctive therapy in patients having major depressive disorder (MDD) with significant anxiety symptoms, 6 did not meet the criterion for efficacy vs placebo. Although 6 showed efficacy signals on several anxiety and depression measures, the primary end point was

not met and overall the results did not suggest efficacy for **6** as an adjunctive treatment for patients with MDD with significant anxious symptoms. ¹⁶⁻²²

To understand more about the key *in vitro* parameters that could drive *in vivo* efficacy, we have focused on the ligand binding kinetics in addition to more classical *in vitro* parameters. It is now becoming increasingly apparent that *in vivo* efficacy can depend on optimized kinetic behavior.²³ Indeed, in the last decade the concept of ligand binding kinetics has received an increasing amount of interest.^{24–27} Both the association and dissociation rate constants k_{on} and k_{off} have been studied for various drug targets including GPCRs.²⁸ The relevance of residence time (RT), defined as the reciprocal of the dissociation rate constant (RT = $1/k_{off}$), for *in vivo* efficacy was retrospectively shown for multiple marketed GPCR drugs, such as the long acting M_3 receptor antagonist tiotropium and fast dissociating D_2 antagonists with lower side-effect burden.^{29–31} Whereas dissociation rates have been the focus of most kinetic studies, association rates have also been described to be important for fast drug action and high receptor occupancy.^{32–34}

Figure 1. Structures of reference $mGlu_2$ PAMs. The position of the tritium label of [3H]JNJ-46281222 (7) is denoted by *.

Here, we report the synthesis and biological evaluation of a novel series of 7-aryl-1,2,4-triazolo[4,3-a]pyridines, which evolved from a pyridone series (4 and 6) through a scaffold hopping drug-design strategy previously described.^{35,36} These compounds were characterized as mGlu₂ PAMs in a functional assay and additionally, radioligand binding experiments were performed to determine their affinity and kinetic binding parameters. We demonstrate that the differentiated binding kinetics result in a varied response in a label-free assay on whole cells. In this way we have been able for the first time to obtain both structure-activity/affinity relationships and structure-kinetic relationships for a class C GPCR.

CHEMISTRY

The target compounds 8–48 were prepared via Suzuki cross coupling of the corresponding 7-halotriazolopyridines (49a,b; 50a-c and 51a,b) with an array of boronic esters (52a-v) as shown in Scheme 1. The chemical structures of compounds 8–48 are shown in Tables 3-6).

The key 7-halotriazolopyridines (**49a,b**; **50a-c** and **51a,b**) and non-commercially available boronic esters (**52a-v**) were prepared following the procedures previously described.^{37,38}

Scheme 1. Synthesis of Final Compounds 8 - 48^a

```
49a: R^1 = °propylmethyl; R^2 = CF_3; X = CI 49b: R^1 = ethoxymethyl; R^2 = CF_3; X = CI 50a: R^1 = °propylmethyl; R^2 = CI; X = I 50b: R^1 = ethoxymethyl; R^2 = CI; X = I 50c: R^1 = trifluoroethyl; R^2 = CI; X = I 51a: R^1 = °propylmethyl; R^2 = I Me; I = I = °propylmethyl; I = °propyl; I = I = °propylmethyl; I = °propyl; I = I = °propyl; I = I = °propylmethyl; I = °propyl; I = I = °propyl; I = I = °propylmethyl; I = °propylmeth
```

```
52a: R^3 = 2.6-dimethylpyridyl-3-oxy; R^4 = F
52b: R^3 = 2.6-dimethylpyridyl-3-oxy: R^4 = CI
52c: R^3 = 2-methylpyridyl-4-oxy; R^4 = F
52d: R^3 = 2-ethylpyridyl-4-oxy; R^4 = F
52e: R^3 = 2.6-dimethylpyridyl-4-oxy; R^4 = F
52f: R^3 = 2^{-c}propylpyridyl-4-oxy: R^4 = F
52g: R^3 = {}^{i}propylamino; R^4 = F
52h: R^3 = {}^{i}propylamino; R^4 = CI
52i: R^3 = {}^{c}propylamino: R^4 = F
52i: R^3 = ^{c}propylamino; R^4 = CI
52k: R<sup>3</sup> = 2-methoxypyridyl-5-methyloxy; R<sup>4</sup> = F
52I: R^3 = 2-methoxypyridyl-5-methyloxy: R^4 = H
52m: R^3 = 3-methoxypyridyl-5-methylamino; R^4 = F
52n: R<sup>3</sup> = 3-methoxypyridyl-5-methylamino; R<sup>4</sup> = H
52o: R<sup>3</sup> =tetrahydro-pyranyl-4-oxy: R<sup>4</sup> = CI
52p: R<sup>3</sup> =tetrahydro-pyranyl-4-amino; R<sup>4</sup> = CI
52q: R<sup>3</sup> =tetrahydro-pyranyl-4-aminomethyl; R<sup>4</sup> = CI
52r: R<sup>3</sup> = trans-4-hydroxy-cyclohexylamino; R<sup>4</sup> = CI
52s: R<sup>3</sup> = cis-4-hydroxy-cyclohexylamino; R<sup>4</sup> = CI
52t: R^3 = cis - 4 - {}^{c}propvl - 4 - hydroxy - cyclohexylamino: <math>R^4 = CI
52u: R<sup>3</sup> = trans-4-hydroxy-cyclohexyloxy; R<sup>4</sup> = CI
52v: R^3 = cis - 4-hydroxy-cyclohexyloxy; R^4 = CI
```

^a Reagents and conditions: (a) Pd(PPh₃)₄, NaHCO₃, H₂O/1,4-dioxane, 150°C, 5-30 min, microwave.

BIOLOGY

The potency of the compounds was determined by quantifying the increase in response of a fixed EC₂₀ glutamate concentration (4 μ M) observed in a functional [35S]GTP γ S binding assay. The affinity of all compounds was determined in a full curve radioligand displacement assay in the presence of 6 nM of the mGlu, PAM 3-(Cyclopropylmethyl)-7-[(4-phenyl-1-piperidinyl)methyl]-8-(trifluoromethyl)-1,2,4-triazolo[4,3-a]pyridine (7, JNJ-46281222), which was radioactively labelled with tritium and extensively characterized in chapter 2.39 In order to determine the kinetic parameters k_{on} and k_{off} we performed a radioligand competition association assay characterized by the equations of Motulsky and Mahan that describe the binding between two ligands competing for the same receptor binding site. 40 For this purpose, first the association rate constant k_{off} and dissociation rate constant k_{off} of 7 were determined in radioligand association and dissociation experiments using a scintillation proximity assay (SPA).41 Kinetic parameters were determined at 28°C, presumably these will increase at 37°C. All kinetic assays were performed in the presence of 1 mM glutamate; as was shown in chapter 2, this condition induced a monophasic association process of the PAM, which is required for the determination of the kinetic parameters of unlabeled PAMs.³⁹ Chapter 2 also showed that the presence of glutamate was shown to not affect affinity and kinetic parameters of 7.39 Ultimately, three compounds with representative RT values were selected for comparison in a label-free, impedance based assay (xCELLigence) which measures ligand-induced responses on whole cells. This assay provided further understanding of the influence of RT on the duration of PAM-induced receptor activation.

RESULTS AND DISCUSSION

Kinetic rate constants k_{on} and k_{off} for 7 were similar when obtained in the association and dissociation assays compared to the competition association assay (Table 1), which validated the use of the competition association assay for all other compounds. Kinetic K_D values were comparable to the values reported in **chapter 2**.³⁹

Reference mGlu₂ PAMs **2-5** (Table 2) showed moderate to good potency and affinity at the mGlu₂ receptor, in agreement with previous reports including **chapter 2**. ^{39,42,43} Kinetic parameters k_{on} , k_{off} and RT were also determined. Reference compound **2** was shown to have a RT of 11.6 minutes. The other reference PAMs had RTs in the same range, from 7.8 minutes for **5** to 17.3 minutes for **7** (Table 1).

Table 1. Comparison of kinetic parameters of compound 7 determined by two different methods^a

Assay	K_{D} (nM) b	k _{on} (M ⁻¹ min ⁻¹)	k _{off} (min ⁻¹)	RT (min)
Association and dissociation ^c	1.1 ± 0.22	$(7.1 \pm 0.43) \times 10^7$	0.080 ± 0.015	12.5 ± 2.3
Competition association ^d	2.5 ± 0.71	$(2.3 \pm 0.60) \times 10^7$	0.058 ± 0.005	17.3 ± 1.6

^aValues represent the mean \pm SEM of at least three individual experiments performed in duplicate. ^bKinetic K_D values, defined by $K_D = k_{off} / k_{on}$. 'Association and dissociation rate constants of [³H]-7 in a classical radioligand kinetic binding assay at 28°C using SPA. ^dAssociation and dissociation rate constants of 7 measured in a competition association assay using SPA at 28°C.

Table 2. Functional activity (pEC₅₀), affinity (pK_i and K_p) and kinetic parameters (k_{on} , k_{off} RT) for reference mGlu₂ PAMs 2-5

	pEC ₅₀	pK _i ^b	k _{on} (M ⁻¹ min ⁻¹) ^c	k_{off} (min ⁻¹) ^d	RT (min) ^e	K_{D} (nM) ^f
2	7.03 ± 0.14 ^a	7.22 ± 0.15	$(4.6 \pm 2.3) \times 10^6$	0.086 ± 0.022	11.6 ± 2.9	190 ± 100
3	6.97 ± 0.08^a	7.10 ± 0.04	$(1.2 \pm 0.38) \times 10^6$	0.120 ± 0.020	8.4 ± 1.4	100 ± 36
4	7.1 ± 0.1°	7.58 ± 0.08	$(1.7 \pm 0.70) \times 10^6$	0.090 ± 0.015	11.1 ± 1.9	51 ± 22
5	6.25 ± 0.06	6.43 ± 0.03	$(2.1 \pm 0.65) \times 10^{5}$	0.128 ± 0.040	7.8 ± 2.4	600 ± 260

As previously described in a Farinha et al. (2015)⁴², b Chapter 2³⁹. cd,e,f Values represent the mean \pm SEM of at least three individual experiments. e RT = $1/k_{off}$ f Kinetic K_D values, defined by $K_D = k_{off} / k_{of}$.

The analysis of the triazolopyridines containing a substituted pyridine (Table 3) began with elaboration of the R^1 substitution. Compound 8 was taken as the starting point. Substitution of chlorine at the R^1 position by trifluoromethyl (9) resulted in an increase in potency, while affinity remained the same. Introduction of methyl (10) or iso-propyl (11) led to an approx. 10-fold decrease in affinity and potency. Interestingly both k_{on} and RT values were similar for 8, 10 and 11 but 2-fold (k_{on}) and approx. 3-fold (RT) higher for 9. Substitution of fluorine by chlorine at the R^2 position resulted in increased potency and affinity for 12, 13 and 14. In both cases, the PAMs with CF_3 at R^1 (9 and 13) showed modestly longer RTs of 30 and 23 minutes, respectively, along with highest potency and affinity.

Exploration of the pyridine R^3 revealed the importance of the position of the nitrogen. Compound **15** showed decreased potency and affinity compared to **8**. A similar trend was seen for **16** that showed values comparable to those reported previously which revealed decreased potency and affinity compared to **9**. Values for k_{on} followed this trend whereas RTs remained the same for **15**, but decreased from 30 to 11 minutes for **16**. Subsequently the alkyl substituents on the pyridine ring were evaluated. Substitution of methyl in **15** by ethyl in **17**, led to an increased potency and affinity. Addition of a methyl group on the 5-position of **16**, did not change affinity or potency in **18**, nor were large changes seen in kinetic parameters. Introduction of the bulky and lipophilic iso-propyl in **19** and **20** increased potency, affinity and k_{on} slightly. Interestingly, the RT of **20** was reduced to only 5 minutes.

Substitution of the cyclopropylmethyl substituent at the R⁴ position by 2,2,2-trifluoroethyl (21) resulted in a slight decrease in affinity, similar values for potency and RT, and a 5-fold increase in k_{on} compared to 8. Next, the ethoxymethyl substituent was evaluated at R⁴ (22), which yielded a slight decrease in potency, a 10-fold decrease in k_{on} and similar values for affinity and RT compared to 21. Substitution of F in 22 by CF₃ at R¹ did not yield a drastic increase in affinity and potency (23). Together, 21-23 showed that a cyclopropyl methyl substituent at R⁴ is preferred, as in all three cases the analogue bearing cyclopropyl methyl at R⁴ showed a higher affinity (8 or 9).

The structure of substituted pyridine of 8 was changed to the short aliphatic iso- or cyclopropyl substituent, yielding **24-30** (Table 4). Potency and affinity of **24** were relatively low (pEC₅₀ 6.65; pK_i 7.21). Changing the R¹ substituent to CF₃ (**25**) increased affinity and potency again (pEC₅₀ 7.03; pK_i 8.05). Substitution of the fluorine on R² to chlorine (**26**) resulted in a \odot 3-fold increase in affinity and potency.

Substitution of i-Pr at the R³ position by a c-Pr induced an increase in affinity and potency in all cases (27-29). As observed in Table 3, replacing F at R² in 27 by Cl in 30 led to an increased affinity and potency and a concomitant increase in k_{on} . The data in Table 4 show that k_{on} values followed affinity, whereas RT values were all within a narrow range (8.2 – 11.9 min).

Table 3. Functional activity (pEC₅₀), affinity (pK₁ and K_D) and kinetic parameters (k_{or} , k_{or} , RT) for mGlu₂ PAMs 8-23

	R ₁	R ²	R³	\mathbf{R}^4	pEC ₅₀ ª	pK^b_{i}	k _{on} (M⁻¹ min⁻¹) ^c	$k_{_{off}}$ (min ⁻¹) d	RT (min)e	K_{D} (nM) t
00	Ū	ш	Z	CH ₂ -(c-Pr)	7.39 (7.35;7.43)	8.71 ± 0.12	(6.3 ± 1.5) × 10 ⁶	0.097 ± 0.024	10.3 ± 2.5	15.3 ± 5.3
6	CF3	ш	Z	CH ₂ -(c-Pr)	8.06 ± 0.14	8.59 ± 0.10	$(1.3 \pm 0.49) \times 10^7$	0.033 ± 0.009	30.1 ± 8.2	2.5 ± 1.2
10	Me	ш	Z	CH ₂ -(c-Pr)	7.11 (7.02; 7.19)	7.66 ± 0.33	(8.6 ± 3.3) × 10 ⁶	0.086 ± 0.013	11.6 ± 1.8	10.0 ± 4.1
7	-Pr	ш	Z	CH ₂ -(c-Pr)	7.55 (7.55; 7.54)	7.60 ± 0.24	$(6.5 \pm 1.4) \times 10^6$	0.070 ± 0.017	14.2 ± 3.5	10.7 ± 3.5
12	Ū	Ū	2 CI CI CI	CH ₂ -(c-Pr)	7.91 (7.71; 8.11)	8.22 ± 0.13	$(6.2 \pm 2.4) \times 10^7$	0.061 ± 0.009	16.3 ± 2.4	1.0 ± 0.40
13	CF3	Ū	, Z	CH ₂ -(c-Pr)	8.54 (8.31; 8.78)	8.82 ± 0.22	$(6.1 \pm 2.4) \times 10^6$	0.044 ± 0.006	22.7 ± 2.9	7.3 ± 3.0

4	Me	Ū		CH ₂ -(c-Pr)	7.76 ±0.26	7.83 ± 0.25	$(5.5 \pm 1.7) \times 10^6$	0.096 ± 0.021	10.5 ± 2.3	17.4 ± 6.5
•	U	щ	z	CH ₂ -(c-Pr)	6.60 (6.64; 6.55)	7.20 ± 0.14	$(2.6 \pm 0.72) \times 10^6$	0.096 ± 0.031	10.4 ± 3.4	37.6 ± 16
	G.	щ	z	CH ₂ -(c-Pr)	7.25 ± 0.32	8.15 ± 0.05	$(9.8 \pm 5.2) \times 10^6$	0.090 ± 0.015	11.1 ± 1.8	9.2 ± 5.1
	Ū	щ	z z	CH ₂ -(c-Pr)	7.00 ± 0.10	7.73 ± 0.08	$(3.0 \pm 0.97) \times 10^6$	0.069 ± 0.011	14.4 ± 2.3	23.3 ± 8.4
	P.	щ	z 	CH ₂ -(c-Pr)	7.19 ± 0.10	8.00 ± 0.16	(8.3 ± 0.60) x 10 ⁶	0.095 ± 0.020	10.5 ± 2.2	11.5 ± 2.5
	Ū	ш	Z *	CH ₂ -(c-Pr)	7.06 ± 0.07	7.27 ± 0.20	$(1.7 \pm 0.82) \times 10^6$	0.073 ± 0.004	13.7 ± 0.8	42.7 ± 21
	G.	ш	Z *	CH ₂ -(c-Pr)	7.73 ± 0.14	8.44 ± 0.07	$(2.2 \pm 0.42) \times 10^7$	0.189 ± 0.082	5.3 ± 2.3	8.6 ± 4.1
	Ū	ш	Z	CH ₂ -CF ₃	7.53 ± 0.11	8.10 ± 0.24	$(2.9 \pm 0.49) \times 10^7$	0.096 ± 0.013	10.5 ± 1.5	3.3 ± 0.7
	Ū	щ	Z	CH ₂ -OEt	7.13 (7.27; 6.99)	8.19 ± 0.10	$(3.0 \pm 0.11) \times 10^6$	0.076 ± 0.004	13.2 ± 0.7	25.2 ± 1.6
	CF ₃	ட	. N	CH ₂ -OEt	7.53 ± 0.19	7.93 ± 0.26	$(3.6 \pm 2.1) \times 10^7$	0.075 ± 0.006	13.4 ± 1.0	2.1 ± 1.2

 a Values represent the mean followed by individual values in parentheses when of two experiments and the mean \pm SEM when of three or more experiments. hcd,ac Values represent the mean \pm SEM of at least three individual experiments, all performed in duplicate. a RT = 1 l l l Kinetic b values, defined by b b a b l b a b b c $^{$

Table 4. Functional activity (pEC₅₀), affinity (pK₁ and K_{D}) and kinetic parameters (k_{on} , k_{orr} RT) for mGlu₂ PAMs 24-30

	٣.	R ₂	R³	pEC ₅₀ ª	pKi	k _{on} (M⁻¹ min⁻¹) ^c	$k_{o\#}$ (min ⁻¹) d	RT (min) ^e	K_{D} (nM) f
24	Ū	ш	i-Pr	6.65 (6.43; 6.88)	7.21 ± 0.07	$(5.0 \pm 1.2) \times 10^6$	0.101 ± 0.009	9.9 ± 0.9	20.3 ± 5.4
25	P.	ш	i-Pr	7.03 (7.44; 6.62)	8.05 ± 0.10	$(4.6 \pm 1.1) \times 10^7$	0.100 ± 0.029	10.0 ± 2.9	2.2 ± 0.8
56	G.	Ū	i-Pr	7.76 (7.55; 7.96)	8.41 ± 0.07	$(3.6 \pm 1.3) \times 10^7$	0.121 ± 0.035	8.2 ± 2.4	3.4 ± 1.6
27	Ū	ш	27 Cl F c-Pr	7.20 (7.19; 7.21)	7.99 ± 0.05	$(4.8 \pm 1.5) \times 10^6$	0.061 ± 0.006	16.4 ± 1.7	12.7 ± 4.1
28	P.	ш	c-Pr	7.52 (7.60; 7.43)	8.44 ± 0.07	$(7.7 \pm 4.8) \times 10^7$	0.086 ± 0.018	11.9 ± 2.3	1.1 ± 0.7
59	P.	Ū	c-Pr	8.11 (8.04; 8.18)	8.65 ± 0.11	$(7.7 \pm 3.8) \times 10^7$	0.088 ± 0.007	11.3 ± 0.9	1.2 ± 0.6
30	Ū	Ū	c-Pr	7.53 (7.54; 7.51)	8.17 ± 0.03	$(1.4 \pm 0.35) \times 10^7$	0.084 ± 0.016	11.9 ± 2.3	6.1 ± 1.9

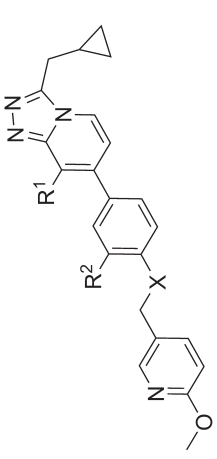
 a Values represent the mean followed by individual values in parentheses. $^{b_{c}c_{d}c_{l}}$ Values represent the mean \pm SEM of at least three individual experiments. e RT = $1/k_{off}$ Kinetic K_{b} values, defined by $K_{p} = k_{off}/k_{off}$.

In addition to the results obtained with the first sub-series of triazolopyridines 8-23, a 4-methoxy-3-pyridine moiety connected by a methylene spacer was introduced, leading to compounds 31-35 (Table 5). These molecules share a moderate to good potency and affinity (pEC₅₀ 6.8 – 7.8; pK₁ 7.9 – 8.7). Removal of the fluorine at the R² position (32) did not significantly change affinity, potency or kinetic parameters when compared to 31. Changing the ether linker in 31 and 32 to an amine in 33 and 34 resulted in an approx. 3-fold increase in affinity and potency. A moderate increase in k_{on} was observed and interestingly a 4- and 2-fold increase in RT for 33 and 34, respectively. This may be explained by the increased flexibility given by the methylene bridge between the triazolopyridine core and the pyridine substituent. As seen in many examples, substitution of CF₃ in 34 to Cl in 35 led to a decrease in affinity, potency and kinetic parameter values.

Reducing aromaticity and introducing more aliphatic and sp3 character can sometimes be beneficial for physicochemical properties and drug-likeness. In order to evaluate the effects of aromaticity, the 4-methoxy-3-pyridyl substituent was replaced with a 4-tetrahydropyranyl ring (36, Table 6). This change resulted in a (pK_i) and potency (pEC₅₀) of 6.65 and 7.64, respectively, which were increased in 37 by the introduction of CF₃ in the R¹ position. Compound 37 has a high affinity (pK_i 8.28) and increased k_{on} (2.0 x $10^7 \,\mathrm{M}^{-1}\mathrm{min}^{-1}$), however, contrary to the high affinity, its RT (4.1 min) was the shortest found throughout this study. As seen in the first series of ligands (Table 2), affinity and potency did not change by altering the linker atom from ether to amine (38, 39). Increasing the linker length by a single methylene unit resulted in an approx. 10-fold loss in affinity, (40; pK_i 7.21). Values for k_{on} followed affinity, but RT values were all in the same range.

The tetrahydropyran moiety was then replaced by a cyclohexanol ring, leading to 41-48. Again, compounds bearing CF₃ at R¹ (42, 46) showed better affinity and potency than their chlorine analogues (41, 45). Molecule 42 not only showed a high potency (pEC₅₀ 8.03), affinity (pK₁ 8.66) and k_{on} (1.1 x 10⁷ M¹min¹), but also a longer RT of 31 minutes. Its cis-diastereomer 43 showed a 3-fold reduction in potency (pEC₅₀ 7.38) and affinity (pK₁ 8.03), a 2-fold reduction in k_{on} (5.7 x 10⁶ M¹min¹) and a small reduction in RT (17 min). Introduction of a c-Pr substituent at R³ (44) led to an increase in potency (pEC₅₀ 8.95), affinity (pK₁ 9.05) and k_{on} (1.4 x 10⁷ M¹min¹), and also to a prolonged RT of 50 minutes, which was the highest value observed in this study. It may be that the cyclopropyl at R³ directs the hydrophilic hydroxyl into a better position for interaction with the receptor. Changing R⁴ from c-Pr to CF₃ (45) did not change any parameter compared to 41. Changing the linker group from amine in 43 to ether in 46 did not affect affinity and potency. However, RT seemed to be somewhat increased. Differences between diastereomers were seen again in 47 and 48. Whereas the potencies were similar, affinity was decreased 3-fold and k_{on} remained similar, while RT was prolonged by 2-fold when moving from a *trans* to *cis* configuration.

Table 5. Functional activity (pEC₅₀), affinity (pK_, and K_{ρ}) and kinetic parameters (k_{oo} , k_{oo} , k_{oo} , k_{oo} , k_{oo} , and k_{oo} are k_{oo} and k_{oo} and k_{oo} are k_{oo} and k_{oo} are k_{oo} and k_{oo} and k_{oo} are k_{oo} and k_{oo} are k_{oo} and k_{oo} are k_{oo} and k_{oo} and k_{oo} are k_{oo} and k_{oo} and k_{oo} are k_{oo} and k_{oo} are k_{oo} and k_{oo} are k_{oo} and k_{oo} and k_{oo} are k_{oo} and k_{oo} are k_{oo} and k_{oo} are k_{oo} and k_{oo} and k_{oo} are k_{oo} and k_{oo} and k_{oo} are k_{oo} and k_{oo} are k_{oo} and k_{oo} and



	R,	\mathbb{R}^2	×	pEC ₅₀ ª	pK^b_{i}	k_{on} (M ⁻¹ min ⁻¹) ^c	$k_{_{off}}$ (min ⁻¹) d	RT (min) ^e	K_{D} (nM) f
31	CF ₃	ш	0	7.39 (7.40; 7.37)	7.93 ± 0.14	$(1.1 \pm 0.40) \times 10^7$	0.173 ± 0.007	5.8 ± 0.2	16.0 ± 5.9
32	P.	I	0	7.24 ± 0.07	8.06 ± 0.16	$(1.4 \pm 0.86) \times 10^7$	0.125 ± 0.013	8.0 ± 0.8	8.7 ± 5.4
33	P.	ш	ĭ	8.23 (8.13; 8.33)	8.69 ± 0.16	$(1.5 \pm 0.94) \times 10^7$	0.044 ± 0.005	22.7 ± 2.8	2.9 ± 1.9
34	P.	I	ĭ	7.82 ± 0.05	8.50 ± 0.09	$(3.4 \pm 1.3) \times 10^7$	0.069 ± 0.012	14.6 ± 2.6	2.0 ± 0.8
35	U	Ŧ	ĭ	6.82 (6.94; 6.71)	8.13 ± 0.08	$(6.2 \pm 1.6) \times 10^6$	0.097 ± 0.022	10.3 ± 2.3	15.6 ± 5.3

 $^{\circ}$ Values represent the mean followed by individual values in parentheses when of two experiments and the mean \pm SEM when of three or more experiments. b,cd,c,f Values represent the mean \pm SEM of at least three individual experiments, all performed in duplicate. c RT = 1/ k_{off} Kinetic K_{D} values, defined by $K_{D} = k_{off} I k_{off}$

Table 6. Functional activity (pEC_{so}), affinity (pK, and K_p) and kinetic parameters ($k_{o,r}, k_{o,r}$ RT) for mGlu₂ PAMs 36-48

R-N-N-N-R4		.
pu	ó ×	R ² / 3

	~	%	<u>~</u>	\mathbb{R}^4	×	>	pEC ₅₀ ª	pK _i ^b	k _{on} (M ⁻¹ min ⁻¹) ^c	$k_{_{off}}$ (min ⁻¹) d	RT (min) ^e	$K_{_D}$ (nM) $^{\prime}$
36	J	,		CH ₂ -(c-Pr)	0	0	6.65 (6.54; 6.77)	7.64 ± 0.01	$(3.3 \pm 1.4) \times 10^6$	0.092 ± 0.014	10.9 ± 1.7	28.1 ± 13
37	CF ₃	1	1	CH ₂ -(c-Pr)	0	0	7.42 (7.40; 7.45)	8.28 ± 0.18	$(2.0 \pm 0.61) \times 10^7$	0.241 ± 0.063	4.1 ± 1.1	12.3 ± 5.0
38	U	ı	ı	CH ₂ -(c-Pr)	ĭ	0	6.83 (6.77; 6.89)	7.41 ± 0.21	$(7.0 \pm 2.4) \times 10^6$	0.136 ± 0.023	7.3 ± 1.2	19.5 ± 7.5
39	CF ₃	1	1	CH ₂ -(c-Pr)	ĭ	0	7.73 (7.77; 7.68)	8.30 ± 0.06	$(1.8 \pm 0.61) \times 10^7$	0.067 ± 0.008	15.0 ± 1.8	3.8 ± 1.4
40	GF ₃	ı	ı	CH ₂ -(c-Pr)	CH ₂ -NH	0	6.20 (6.23; 6.18)	7.21 ± 0.06	$(1.7 \pm 0.18) \times 10^6$	0.091 ± 0.018	11.0 ± 2.1	54 ± 12
41	ō	I	ОН	CH ₂ -(c-Pr)	ĭ	O	7.48 ± 0.22	8.52 ± 0.08	$(6.7 \pm 1.3) \times 10^6$	0.084 ± 0.011	11.8 ± 1.6	12.7 ± 3.0
42	GF ₃	I	НО	CH ₂ -(c-Pr)	ĭ	O	8.03 ± 0.12	8.66 ± 0.01	$(1.1 \pm 0.09) \times 10^7$	0.033 ± 0.002	30.8 ± 1.7	3.0 ± 0.3
43	G.	НО	I	CH ₂ -(c-Pr)	ĭ	O	7.38 ± 0.08	8.03 ± 0.17	$(5.7 \pm 1.3) \times 10^6$	0.058 ± 0.014	17.1 ± 4.0	10.3 ± 3.4
44	CF ₃	НО	c-Pr	CH ₂ -(c-Pr)	ĭ	U	8.95 (9.00; 8.90)	9.05 ± 0.10	$(1.4 \pm 0.16) \times 10^7$	0.020 ± 0.005	49.5 ± 12.4	1.5 ± 0.4
45	ō	I	НО	CH ₂ -CF ₃	ĭ	O	7.38 (7.41; 7.34)	8.22 ± 0.20	$(6.7 \pm 1.3) \times 10^6$	0.074 ± 0.015	13.6 ± 2.8	10.8 ± 3.1
46	F.	НО	I	CH ₂ -(c-Pr)	0	O	7.60 (7.64; 7.57)	8.72 ± 0.15	$(1.2 \pm 0.31) \times 10^7$	0.036 ± 0.001	28.1 ± 0.7	3.0 ± 0.8
47	Ū	I	НО	CH ₂ -CF ₃	0	O	6.80 (6.73; 6.88)	7.94 ± 0.04	$(8.3 \pm 3.6) \times 10^6$	0.137 ± 0.049	7.3 ± 1.2	16.6 ± 9.3
48	╗	Н	ェ	CH ₂ -CF ₃	0	U	7.01 (7.03; 6.99)	7.49 ± 0.21	$(6.9 \pm 1.5) \times 10^6$	0.056 ± 0.001	17.7 ± 0.2	8.1 ± 1.7

 $^{\circ}$ Values represent the mean followed by individual values in parentheses when of two experiments and the mean \pm SEM when of three or more experiments. $^{b,cd,c'}$ Values represent the mean \pm SEM of at least three individual experiments, all performed in duplicate. c RT = 1 b c values, defined by b c = b $^{c,d'}$ $^{c,d'}$ $^{c,d'}$ values.

In general, CF₃ was shown to be the preferred substituent at R¹. Compounds bearing this substituent typically had a higher potency and affinity. Interestingly, all PAMs with a RT longer than 20 minutes bear this moiety, including 44 with the longest RT seen in this study (50 min). On the other hand, molecule 37 had the shortest RT (4.1 min) and also contains the CF₃ group, indicating that CF₃ in itself is not the driver for long RT. At the R² position chlorine was shown to be the best substituent for high potency and affinity. PAMs bearing a substituted pyridine revealed the importance of its substitutions in combination with the position of the nitrogen in the ring for potency, affinity and kinetic parameters.

The rather small differences in RT induced by substitutions at the R¹ and R² position at the central triazolopyridine core indicated that this region does not induce large differences in RT. On the other hand, small differences in the distal tail of the compounds induced large differences in RT. As shown in **chapter 2**, this triazolopyridine series binds with the scaffold and R⁴ substituent in the deepest part of the receptor, whilst the distal tail points to the extracellular side.³⁹ These differences in RT may be explained by the tight receptor-ligand interactions of the triazolopyridine core compared to looser interactions on the extracellular side. Certain molecules may trap the more flexible ECL2 (or the tops of TMs 3 and 5) in conformations leading to longer RT. Such induced fit modulation of RT can involve ordering of loops to partially block the binding pocket and prevent ligand escape. This mechanism has been seen for multiple targets from different classes, amongst which the 5-HT_{2B} receptor as reported in the recently published LSD-bound crystal structure.^{24,45} Selectivity of this series of mGlu₂ PAMs for other members of the mGlu family was good. Representatives (**12**, **27**, **37** and **45**) showed no activity at mGlu1, 3, 4, 5, 6, 7 or 8, see table S1.

In order to compare the kinetic parameters and affinity, a kinetic map was generated (Fig. 2). In this map k_{on} (x-axis), k_{off} (y-axis) and K_{D} (diagonal lines) were plotted. Whereas k_{off} values were all within a small range of about one order of magnitude between 0.020 min⁻¹ (44) and 0.241 min⁻¹ (37), k_{on} values were more diverse and were spread over almost two orders of magnitude between 1.7×10^6 M⁻¹min⁻¹ (40) to 7.7×10^7 M⁻¹min⁻¹ (28 and 29). The molecules were plotted per subgroup, as presented in the different tables. This revealed that 8-23 and 24-30 were mostly diverse in on-rates (8-23: $0.17 - 6.2 \times 10^7$ M⁻¹min⁻¹; 24-30: $0.48 - 7.7 \times 10^7$ M⁻¹min⁻¹), whereas 31-35 and 36-48 were more diverse in off-rates (31-35: 0.044 - 0.17 min⁻¹; 36-48: 0.020 - 0.24 min⁻¹), indicating that an increased affinity between close analogues may be achieved by optimizing one kinetic parameter at a time. Interestingly, the five reference mGlu₂ PAMs 2-5 and 7, which are very diverse in structure and affinity, differed mostly in terms of on-rate ($0.21 - 4.6 \times 10^6$ M⁻¹min⁻¹), whereas off-rates were very close (0.086 - 0.13 min⁻¹). As expected, the compounds with the highest affinity either have a long RT (44) or a fast k_{on} (28-29). Ideally, these optimized parameters may be combined leading to an mGlu₂ PAM with even more increased affinity, which would be represented in the top right corner of the kinetic map.

For further comparison, the compounds were arbitrarily divided in short RT (RT < 10 min), medium RT (10 - 20 min) and long RT (> 20 min) (Fig. 2).

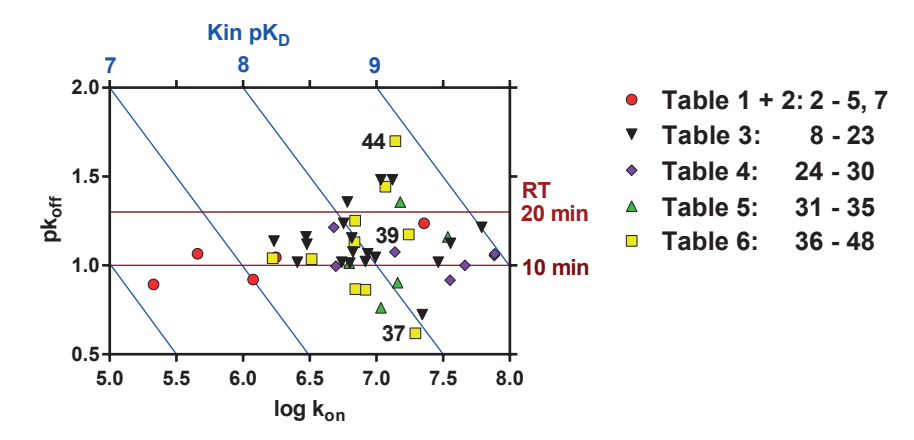


Figure 2. Kinetic map of all tested compounds. The dissociation rate $(pk_{off}, k_{off}, \min^{-1})$ is plotted on the y-axis; the association rate $(\log k_{on}, k_{on}: M^{-1}\min^{-1})$ on the x-axis. Identical affinity (pK_{D}) values may result from a different combination of k_{on} and k_{off} $(K_{D} = k_{off} / k_{on} / k_{on})$ diagonal blue lines). Horizontal lines indicating a RT of 10 and 20 minutes divide the compounds in short, medium and long RT.

To gain more insight in the relationships between the different parameters studied, correlation plots were made (Fig. 3). First, the affinity (pK_i) and potency (pEC₅₀) were shown to be linearly correlated (Fig. 3A). Secondly, the affinity obtained from the classical radioligand displacement assay (pK_i) and affinity obtained from kinetic parameters (pK_D), were shown to be correlated (Fig. 3B). This further supported the use of the kinetic SPA radioligand binding assay. Long RT PAMs were shown to share a high affinity and potency, but by itself a high potency or affinity does not predict a long RT (Fig. 3A, 3B, S1). Then, the dissociation rate constants (pk_{off}) were plotted against the kinetic affinity data (pK_D) (Fig. 3C), which did not show correlation. Interestingly, the association rate constants (log k_{off}) were strongly correlated to affinity (pK_D) (Fig 3D). These parameters were both within a similar range of roughly two orders of magnitude for the compounds of our series. Interestingly, although having different structures and in some cases lower affinities and k_{off} values, the reference mGlu₂ PAMs (2-5) also fitted well in this correlation (Fig. 3D). This indicated that this correlation has likely revealed a general trend for PAMs and how they bind at the mGlu, receptor.

Correlations between kinetic parameters and affinity have been made before. Most of these studies found a correlation between $k_{\rm off}$ values and affinity or efficacy, for instance on the $\rm M_3$ and $\rm A_{\rm 2A}$ receptors. However, a correlation between association rate constants and affinity, as was shown here for mGlu₂ PAMs, has also been observed before. Exemplary GPCRs are the OX₂ receptor and $\rm \beta_2$ -adrenoreceptors, 49,50 and other targets such as the hERG channel. 51,52

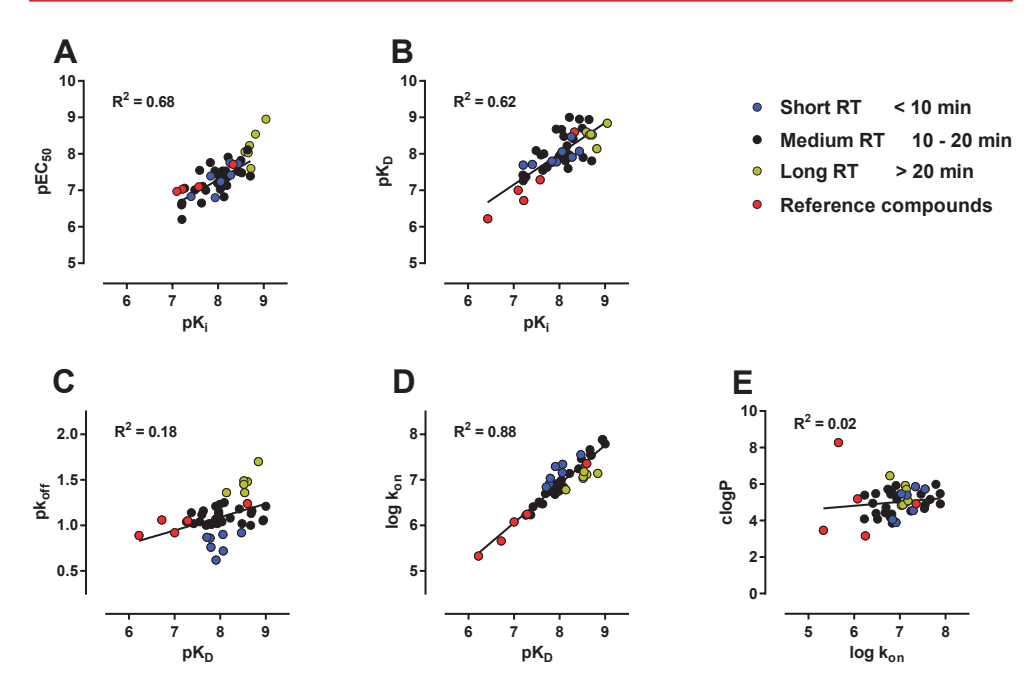


Figure 3. Correlation between affinity (pK_i) and potency (pEC_{so}) (A); affinity determined from [3 H]-**7** displacement assays (pK_i) and affinity determined based on kinetic parameters k_{on} and k_{off} obtained from [3 H]-**7** competition association experiments (pK_D) (B); affinity (pK_D) and dissociation rate (pk_{Off}) (C); affinity (pK_D) and association rate (log k_{on}) (D); association rate (log k_{on}) and partition coefficient (clogP) (E).

These correlations are receptor-specific and may therefore be caused by differences in receptor structure, dynamics, or local environment of the receptor.

Recent simulation studies have stipulated the importance of fast association rates for receptor occupancy and drug dosing.^{33,53} One of the mechanisms which may be responsible for these effects is receptor rebinding, which is described as the binding of freshly dissociated ligands from the local environment of the receptor.⁵⁴ These high local concentrations may lead to a prolonged activity of the drug, even when concentrations within the effect compartment have fallen below therapeutic levels.⁵⁵ For the mGlu₂ receptor, rebinding may play a role. The physiological synaptic environment of the receptor may permit more rebinding as its interstitial location will result in less diffusion and therefore higher local ligand concentrations.^{56,57} Another reason for receptor rebinding would be binding of compound to or in the cell membrane close to the receptor which may then act as a repository and facilitate the approach of the compound to the receptor.⁵⁶ This would, however, require a correlation between lipophilicity and association rate constants, as lipophilic compounds are more likely to bind to the cell membrane. Since the plot in figure 3E shows no such correlation for the studied mGlu₂ PAMs, membrane binding is not likely to be involved for these compounds.

xCELLigence

We used a label-free, impedance-based technology (xCELLigence) to evaluate whether a long receptor binding RT leads to a prolonged functional activity. This method is based on the measurement of cellular impedance, expressed as Cell Index, and enables real-time recordings.58 Responses induced by compound addition can thus be measured and quantified. Earlier studies have shown that results obtained were comparable to more classical endpoint assays.⁵⁹ As the assay is performed on whole cells at 37°C it is considered a valuable translational step towards in vivo experiments.⁶⁰ Endogenous glutamate levels at time of experiments were around 90 µM. Compound-induced responses therefore represent the PAM effects. As a control, reference compound 7 was used to check the response on CHO-K1 WT cells compared to CHO-K1_hmGlu, cells (Fig. S2). No response was found on the WT cells, indicating that the responses were mGlu, receptor-mediated. For further experiments we selected compounds with diversity in RT (measured at 28°C): 37 (4.1 min), its close analogue 39 with 3-4 -fold longer RT (15 min) and 44 with again a 3-fold longer RT compared to 39 (50 min; Fig. 4A-D). We determined their potency in the label-free assay using CHO-K1_ hmGlu₂ cells and found pEC₅₀ values of 7.05 \pm 0.04, 7.73 \pm 0.23 and 7.95 \pm 0.12, respectively. Then we performed a wash-out assay, in order to evaluate differences in compound-induced responses after washing. This enabled us to trace the remaining response exerted by only receptor-bound compound. To this end we first determined the EC_{so} concentrations of short RT 37, medium RT 39 and long RT 44, which were 600, 200 and 60 nM, respectively. Then, cells were stimulated with this EC₈₀ concentration and just before maximal response was reached, after 5 minutes, cells were washed and fresh medium was added (Fig. 4E-G). By comparing these traces with control traces of unwashed wells, we evaluated the differences in responses between 37, 39 and 44 as the ratio between the AUC of washed and unwashed wells (Fig. 4H). The functional effect of 37 and 39 were partially lost in this experimental set-up, while the effect of 44 remained almost unchanged. The wash-out assay showed a significant difference between short RT 37 and long RT 44. The value for 39 was in between those of 37 and 44, in agreement with its RT. Together, these data showed that a longer RT also leads to an increased functional effect under non-equilibrium conditions and that these parameters are positively correlated. Since equilibrium conditions are not always present in physiological conditions, these findings may be considered a translational step from in vitro towards in vivo experiments.

In vivo sleep-wake effects

Glutamate neurotransmission plays a key role in sleep-wake mechanisms and these processes have translational value for central activity and target engagement. Previous *in vivo* studies have repeatedly shown that positive allosteric modulation of the ${\rm mGlu_2}$ receptor results in distinct changes in rodent sleep-wake organization, more specifically in a dose-dependent reduction in so-called Rapid Eye Movement Sleep or REM sleep.^{61,62} Changes in sleep-wake

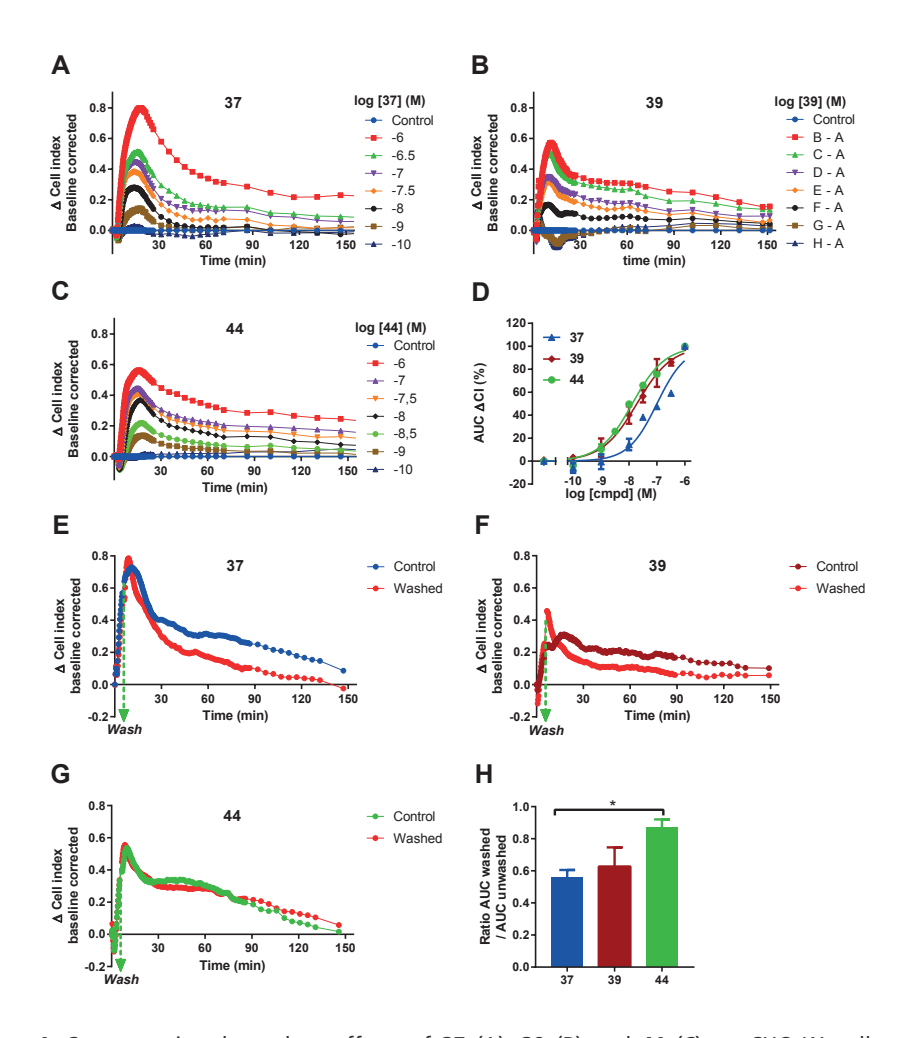


Figure 4. Concentration-dependent effects of 37 (A), 39 (B) and 44 (C) on CHO-K1 cells stably expressing the human ${\rm mGlu}_2$ receptor. A representative example is shown of a baseline-corrected response, which was repeated three times in duplicate. (D) Concentration-effect curve of 37, 39 and 44, derived from the AUC up to 150 minutes. Data are from three individual experiments performed in duplicate and are expressed as percentage of maximum AUC. Responses in a label-free, impedance-based assay induced by an EC₈₀ equivalent concentration of 37 (600 nM) (E), 39 (200 nM) (F) and 44 (60 nM) (G) with and without washing-step induced 5 minutes after stimulation. A representative example is shown of a baseline-corrected response, which was repeated three times in duplicate. (H) Ligand-induced response that is left after washing step. Data are expressed as the ratio between the AUC of the trace of the washed and unwashed wells. Data are from three individual experiments performed in duplicate and are expressed as the mean \pm SEM. * p < 0.05.

states in the rat are of a dynamic nature, i.e. with more frequent transitions between sleep-wake states as compared to humans: therefore the effects of mGlu₂ PAM compounds on REM sleep are expressed as averages over for example 2 hour or 4 hours periods after compound administration. In order to investigate whether the different RT values are reflected in the sleep-wake related pharmacodynamic read-out, sleep-wake analysis of 9 and 20 (selected as

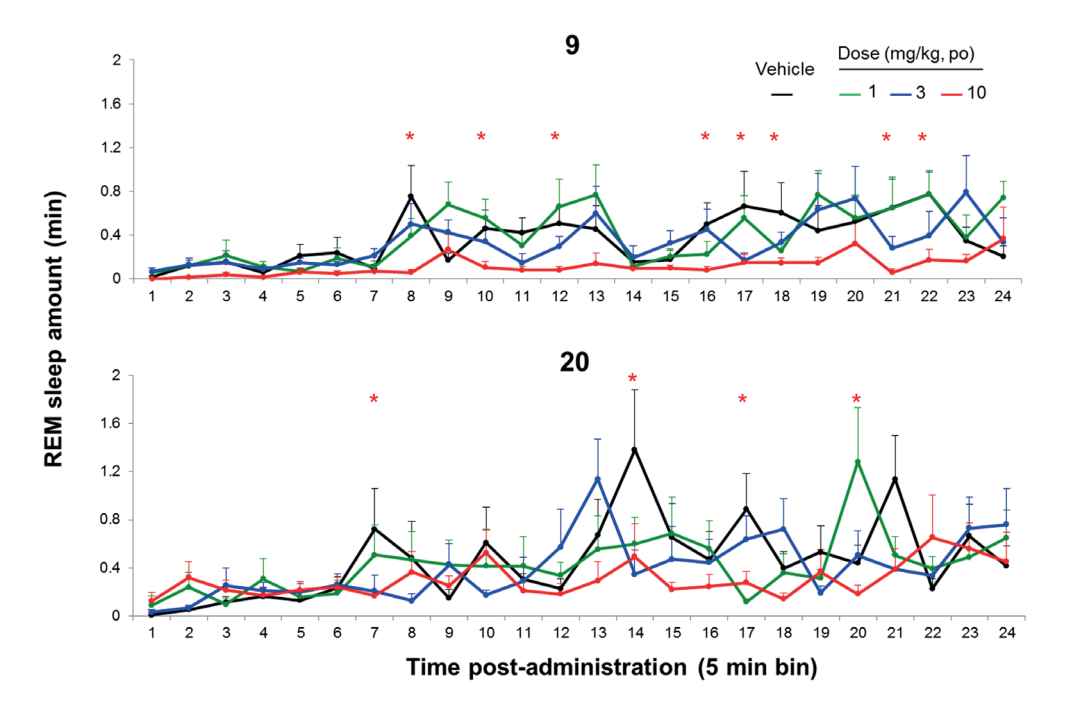


Figure 5. Average amount of REM sleep in minutes for 24 consecutive 5-min period during the first 2 hours of the recording session after oral administration of **9** (top panel) and **20** (bottom panel), each at 1, 3, 10 mg/kg, p.o. to Sprague-Dawley rats (n=8 for each condition). Black lines indicate control vehicle condition (20% CD), while the green, blue, and red lines indicate doses 1, 3, 10 mg/kg, respectively. Error flags indicate SEM values: please note that the higher time resolution of 5 minute bins also causes REM sleep changes to be expressed more dynamically and less 'consistent' as compared to reduction score averaged over the whole 2 hour post-administration period. * indicate p < 0.05 vehicle compared to 10 mg/kg, Mixed Model ANOVA.

examples with long versus short *in vitro* RT, respectively, yet having appropriate and similar pharmacokinetic behavior) was even done on a 5 minute basis to optimally capture sleep changes in function of time. All methods, (circadian) timings and analyses otherwise were similar to those reported earlier by Ahnaou et al. (2016).⁶²

Figure 5 shows the effects of 9 and 20 on REM sleep reduction in rats for 24 consecutive 5-min periods after a single oral administration of 1, 3, and 10 mg/kg and 20% CD vehicle control. The first 6 consecutive 5-minute periods can be discarded due to the confounding arousing effect of the oral administration procedure per se, the animal returning to undisturbed REM sleep baseline values after about 30 minutes. Molecule 9 showed a longer *in vitro* RT of 30 minutes whilst for 20 it was 5 minutes. Correspondingly, at the higher dose of 10 mg/kg, the effect of 9 on REM reduction seemed more immediate and constant compared to 20. For both compounds no effects on total sleep were seen.

Compound 9 and 20 showed similar *in vitro* binding affinities with pK_i values of 8.59 and 8.44, respectively. At 10 mg/kg, estimated free levels in brain 1 hour post-administration are 5 and 3.5 ng/g for 9 and 20, respectively. Hence the two molecules show similar affinity and roughly similar range of free concentrations in brain. While the underlying mechanism causing this different *in vivo* effect is still to be elucidated, this finding provides a first hint that different RT's may impact the *in vivo* effect. The interplay of RT with elimination/clearance from brain is important for the resulting *in vivo* effect, but with similar levels of 9 and 20 after 1 hour, it seems that RT may play a role in this case. To strengthen these observations, future experiments could include the synthesis of PET ligands with different residence times and further *in vivo* studies with a different endpoint such as cognition.

While potent GPCR antagonists can act via a long RT with expected improved clinical efficacy there is limited published data assessing the relationship between agonist/PAM RT and *in vivo* efficacy. Agonist responses are usually regulated by receptor desensitization and internalization, which can act to limit the effect and duration of receptor signaling. PAMs do not activate receptors in the absence of agonist, and hence allosteric modulators with prolonged action may not be negated by internalization and loss of function due to longer RT of the PAM-receptor complex.

CONCLUSIONS

In this study we described a series of 7-aryl-1,2,4-triazolo[4,3-a]pyridines with potent ${\rm mGlu}_2$ PAM activity and a high affinity. An SPA radioligand binding assay was developed to study the kinetic parameters of these compounds. We showed that association rate constants range within three orders of magnitude, whereas RT values are more confined, from 4.1 minutes (37) up to 50 minutes (44). Correlation plots between affinity and kinetic parameters revealed a strong correlation between affinity and association rate constants, whereas no such correlation was found between RT and affinity.

Structure-kinetics relationships were explored in addition to the more traditional structure-activity/affinity relationships analysis. We learned that a CF₃ substituent at R¹ increased potency and affinity and was also important for RT, but did not lead to a long RT *per se* as shown by its presence in 37 ('short' RT) and 44 ('long' RT). Chlorine was the preferred substituent for R², it increased potency and affinity but not RT. Differences in the distal tail of the molecules, such as small changes in the pyridine moiety or single substitutions to the cyclohexanol, induced the biggest differences in RT. This was exemplified by the introduction of c-Pr in 44, leading to a 3-fold increase in RT compared to 43.

To evaluate whether a long RT also leads to a prolonged functional effect, **37**, **39** and **44** were evaluated in a wash-out assay using the label-free impedance based xCELLigence technique. The response of **44** on whole cells at physiological temperature remained more sustained after washing than that of **37** and **39**. These data suggested that an increased lifetime of the receptor-ligand complex (RT) is correlated to an increased functional effect under non-equilibrium conditions.

Together, these results show for the first time for a class C GPCR that optimization of ligand binding kinetics in addition to potency and affinity is possible. Given that pure PAMs do not exert an effect in the absence of glutamate and are thus less likely to induce on-target toxicity, a long RT seems a promising strategy for these ligands. As rebinding may be involved in mGlu₂ receptor occupancy, a RT for **44** in our system of 50 minutes may be prolonged in the interstitial synaptic environment. Without any on-target toxicity occurring, the design of mGlu₂ PAMs with even longer RTs may be a logical next step. Lastly, a first attempt was made to relate the compound's RT to its *in vivo* pharmacodynamic effect. Ultimately, this study may contribute to the development of compounds with a high affinity and efficacy *in vitro* and *in vivo*, not only for the mGlu₂ receptor but also for other GPCRs.

EXPERIMENTAL SECTION

Chemistry

Unless otherwise noted, all reagents and solvents were obtained from commercial suppliers and used without further purification. Thin layer chromatography (TLC) was carried out on silica gel 60 F254 plates (Merck). Flash column chromatography was performed on silica gel, particle size 60 Å, mesh of 230-400 (Merck) under standard techniques. Microwave assisted reactions were performed in a single-mode reactor, Biotage Initiator Sixty microwave reactor (Biotage), or in a multimode reactor, MicroSYNTH Labstation (Milestone, Inc.). Nuclear magnetic resonance (NMR) spectra were recorded with either a Bruker DPX-400 or a Bruker AV-500 spectrometer (Bruker AG) with standard pulse sequences, operating at 400 and 500 MHz, respectively, using CDCl₃ and DMSO-d₆ as solvents. Chemical shifts (δ) are reported in parts per million (ppm) downfield from tetramethylsilane ($\delta = 0$). Coupling constants are reported in hertz. Splitting patterns are defined by s (singlet), d (doublet), dd (double doublet), t (triplet), q (quartet), quin (quintet), sex (sextet), sep (septet), or m (multiplet). Liquid chromatography combined with mass spectrometry (LCMS) was performed on either a HP 1100 HPLC system (Agilent Technologies) or Advanced Chromatography Technologies system composed of a quaternary or binary pump with degasser, an autosampler, a column oven, a diode array detector (DAD), and a column as specified in the respective methods below. Flow from the column was split to a MS spectrometer. The MS detector was configured with either an electrospray ionization source or an ESCI dual ionization source (electrospray combined with atmospheric pressure chemical ionization). Nitrogen was used as the nebulizer gas. Data acquisition was performed with MassLynx-Openlynx software or with Chemsation-Agilent data browser software. Melting point values are peak values and were obtained with experimental uncertainties that are commonly associated with this analytical method. Melting points were determined in open capillary tubes on a Mettler FP62 apparatus with a temperature gradient of 10 °C/min. Maximum temperature was 300 °C.

Purities of all new compounds were determined by analytical RP HPLC using the area percentage method on the UV trace recorded at a wavelength of 254 nm, and compounds were found to have ≥95% purity unless otherwise specified.

- 8-Chloro-3-cyclopropylmethyl-7-{4-[(2,6-dimethylpyridin-3-yl)oxy]-3-fluorophenyl}[1,2,4]triazolo[4,3-a]-pyridine (8). To a stirred suspension of 50a (1.7 g, 5.09 mmol) and 52a (2.1 g, 6.12 mmol) in a saturated aqueous solution of NaHCO₃ (18 mL) and 1,4-dioxane (36 mL) was added Pd(PPh₃)₄ (0.589 g, 0.51 mmol). The mixture was heated at 150 °C for 10 min under microwave irradiation. The mixture was cooled to room temperature and filtered through a Celite pad. The filtrate was diluted with water (20 mL) and extracted with EtOAc (2 × 15 mL). The organic layer was washed with brine (15 mL), dried over anhydrous Na₂SO₄, and concentrated in vacuo. The crude was purified by flash column chromatography (silica gel, EtOAc in DCM, 0/100 to 20/80) to give the desired product 8 as a white solid (1.3 g, 60%). Mp 207.2 °C. ¹H NMR (500 MHz, CDCl₃) 8 ppm 0.32-0.42 (m, 2H), 0.61-0.69 (m, 2H), 1.17-1.28 (m, 1H), 2.54 (s, 3H), 2.55 (s, 3H), 3.13 (d, *J* = 6.9 Hz, 2H), 6.87 (d, *J* = 6.9 Hz, 1H), 6.92 (t, *J* = 8.4 Hz, 1H), 7.02 (d, *J* = 8.4 Hz, 1H), 7.16 (d, *J* = 8.4 Hz, 1H), 7.25 (d, *J* = 9.2 Hz, 1H), 7.41 (dd, *J* = 11.3, 1.7 Hz, 1H), 7.98 (d, *J* = 6.9 Hz, 1H). LC-MS *m*/*z* 423 [M + H]*, t_p = 2.86 min.
- 8-Trifluoromethyl-3-cyclopropylmethyl-7-{4-[(2,6-dimethylpyridin-3-yl)oxy]-3-fluorophenyl}[1,2,4] triazolo[4,3-a]-pyridine (9). Starting from 49a (0.150 g, 0.54 mmol) and 52a (0.242 g, 0.707 mmol) and following the procedure described for 8, compound 9 was obtained as a white solid (0.139 g, 56%).

 ¹H NMR (400 MHz, CDCl₃) δ ppm 0.31-0.43 (m, 2H), 0.61-0.70 (m, 2H), 1.16-1.30 (m, 1H), 2.53 (s, 3H), 2.55 (s, 3H), 3.15 (d, *J* = 6.7 Hz, 2H), 6.79 (d, *J* = 7.2 Hz, 1H), 6.89 (t, *J* = 8.3 Hz, 1H), 7.01 (d, *J* = 8.3 Hz, 1H), 7.05 (br d, *J* = 8.6 Hz, 1H), 7.14 (d, *J* = 8.3 Hz, 1H), 7.22 (dd, *J* = 10.9, 2.1 Hz, 1H), 8.11 (d, *J* = 7.2 Hz, 1H). LC-MS *m*/*z* 457 [M + H]⁺, t_p = 3.03 min.
- 8-Methyl-3-cyclopropylmethyl-7-{4-[(2, ô-dimethylpyridin-3-yl)oxy]-3-fluorophenyl}[1,2,4]triazolo[4,3-a]-pyridine (10). Starting from 51a (0.250 g, 1.127 mmol) and 52a (0.464 g, 1.35 mmol) and following the procedure described for 8, compound 10 was obtained as a white solid (0.103 g, 23%). Mp 147.4 °C. ¹H NMR (500 MHz, CDCl₃) δ ppm 0.32 0.39 (m, 2H), 0.60 0.67 (m, 2H), 1.16 1.29 (m, 1H), 2.55 (s, 6H), 2.65 (s, 3H) 3.11 (d, *J* = 6.65 Hz, 2H), 6.78 (d, *J* = 7.22 Hz, 1H), 6.93 (t, *J* = 8.38 Hz, 1H), 7.07 (d, *J* = 8.38 Hz, 1H), 7.13 (d, *J* = 8.09 Hz, 1H), 7.23 (dd, *J* = 11.27, 2.02 Hz, 1H), 7.89 (d, *J* = 6.94 Hz, 1H). LC-MS *m*/*z* 403 [M + H]⁺, t_R = 2.07 min.
- 8-Cyclopropyl-3-cyclopropylmethyl-7-{4-[(2,6-dimethylpyridin-3-yl)oxy]-3-fluorophenyl}[1,2,4] triazolo[4,3-a]-pyridine (11). Starting from 51b (0.230 g, 0.93 mmol) and 52a (0.382 g, 1.11 mmol) and following the procedure described for 8, compound 11 was obtained as a white solid (0.269 g, 68%). Mp 166.4 °C. ¹H NMR (400 MHz, CDCl₃) δ ppm 0.29 0.38 (m, 2H), 0.58 0.67 (m, 2H), 0.90 1.00 (m, 2H), 1.14 1.31 (m, 1H), 1.55 1.70 (m, 2H) 2.10 (tt, *J*=8.64, 5.46 Hz, 1H), 2.54 (s, 3H), 2.55 (s, 3H), 3.06 (d, *J*=6.70 Hz, 2H), 6.73 (d, *J*=7.17 Hz, 1H), 6.93 (t, *J*=8.44 Hz, 1H), 7.00 (d, *J*=8.32 Hz, 1H), 7.13 (d, *J*=8.32 Hz, 1H), 7.15 7.20 (m, 1H), 7.32 (dd, *J* = 11.21, 1.97 Hz, 1H), 7.80 (d, *J* = 7.17 Hz, 1H). LC-MS *m*/z 429 [M + H]⁺, t_R = 2.24 min.
- 8-Chloro-3-cyclopropylmethyl-7-{4-[(2,6-dimethylpyridin-3-yl)oxy]-3-chlorophenyl}[1,2,4]triazolo[4,3-a]-pyridine (12). Starting from 50a (0.250 g, 0.75 mmol) and 52b (0.385 g, 0.75 mmol) and following the procedure described for 8, compound 12 was obtained as a white solid (0.100 g, 70%). Mp 182.7 °C. ¹H NMR (400 MHz, CDCl₃) δ ppm 0.31 0.41 (m, 2H), 0.57 0.70 (m, 2H), 1.21 1.33 (m, 1H), 2.51 (s, 3H), 2.56 (s, 3H), 3.13 (d, *J* = 6.94 Hz, 2H), 6.82 (d, *J* = 8.55 Hz, 1H), 6.87 (d, *J* = 6.94 Hz, 1H), 7.03 (d, 1.25 Mz) (d, 1.

- J = 8.32 Hz, 1H), 7.16 (d, J = 8.09 Hz, 1H), 7.37 (dd, J = 8.55, 2.31 Hz, 1H), 7.66 (d, J = 2.31 Hz, 1H), 7.97 (d, J = 7.17 Hz, 1H). LC-MS m/z 439 [M + H]⁺, t_n = 3.08 min.
- 8-Trifluoromethyl-3-cyclopropylmethyl-7-{4-[(2,6-dimethylpyridin-3-yl)oxy]-3-chlorophenyl}[1,2,4] triazolo[4,3-a]-pyridine (13). Starting from 49a (0.2 g, 0.73 mmol) and 52b (0.26 g, 0.72 mmol) and following the procedure described for 8, compound 13 was obtained as a white solid (0.217 g, 61%). Mp > 300°C. ¹H NMR (400 MHz, CDCl₃) δ ppm 0.34 0.41 (m, 2H), 0.62 0.70 (m, 2H), 1.16 1.30 (m, 1H), 2.50 (s, 3H), 2.56 (s, 3H), 3.15 (d, *J* = 6.70 Hz, 2H), 6.79 (d, *J* = 8.09 Hz, 2H), 7.03 (d, *J* = 8.09 Hz, 1H), 7.11 7.19 (m, 2H), 7.49 (d, *J* = 2.31 Hz, 1H), 8.10 (d, *J* = 7.17 Hz, 1H). LC-MS *m*/*z* 473 [M + H]⁺, t_p = 3.22 min.
- 8-Methyl-3-cyclopropylmethyl-7-{4-[(2,6-dimethylpyridin-3-yl)oxy]-3-chlorophenyl]{1,2,4]triazolo[4,3-a]-pyridine (14). Starting from 60a (0.250 g, 0.127 mmol) and 52b (0.464 g, 1.35 mmol) and following the procedure described for 8, compound 14 was obtained as a white solid (0.107 g, 22%). Mp 121 °C.

 ¹H NMR (500 MHz, CDCl₃) δ ppm 0.36 (q, *J* = 5.01 Hz, 2H), 0.58 0.67 (m, 2H), 1.17 1.30 (m, 1H), 2.52 (s, 3H), 2.56 (s, 3H), 2.64 (s, 3H), 3.11 (d, *J* = 6.65 Hz, 2H), 6.78 (d, *J* = 6.94 Hz, 1H), 6.83 (d, *J* = 8.67 Hz, 1H), 7.02 (d, *J* = 8.38 Hz, 1H), 7.13 (d, *J* = 8.09 Hz, 1H), 7.18 (dd, *J* = 8.38, 2.02 Hz, 1H), 7.49 (d, *J* = 2.31 Hz, 1H), 7.89 (d, *J* = 6.94 Hz, 1H). LC-MS *m*/*z* 419 [M + H]*, t_p = 2.23 min.
- 8-Chloro-3-cyclopropylmethyl-7-{4-[(2-methylpyridin-4-yl)oxy]-3-fluororophenyl}[1,2,4]triazolo[4,3-a]-pyridine (15). Starting from 50a (1.71 g, 5.13 mmol) and 52c (1.4 g, 5.67 mmol) and following the procedure described for 8, compound 15 was obtained as a white solid (0.100 g, 70%). Mp > 300°C.

 ¹H NMR (500 MHz, CDCl₃) δ ppm 0.34 0.41 (m, 2H), 0.63 0.70 (m, 2H), 1.18 1.28 (m, 1H), 2.55 (s, 3H), 3.14 (d, *J* = 6.65 Hz, 2H), 6.73 (dd, *J* = 5.78, 2.31 Hz, 1H), 6.78 (d, *J* = 2.31 Hz, 1H), 6.91 (d, *J* = 7.22 Hz, 1H), 7.27 7.34 (m, 1H), 7.36 7.41 (m, 1H), 7.45 (dd, *J* = 10.69, 2.02 Hz, 1H), 8.01 (d, *J* = 6.94 Hz, 1H), 8.41 (d, *J* = 5.78 Hz, 1H). LC-MS *m*/*z* 409 [M + H]⁺, t_n = 2.57 min.
- 8-Trifluoromethyl-3-cyclopropylmethyl-7-{4-[(2-methylpyridin-4-yl)oxy]-3-fluororophenyl}[1,2,4] triazolo[4,3-a]-pyridine (16). Starting from 49a (1.4 g, 5.08 mmol) and 52c (1.84 g, 5.59 mmol) and following the procedure described for 8, compound 16 was obtained as a white solid (0.233 g, 10%). Mp 194.6°C. ¹H NMR (500 MHz, CDCl₃) δ ppm 0.34 0.44 (m, 2 H), 0.61 0.73 (m, 2H), 1.18 1.29 (m, 1H), 2.55 (s, 3H), 3.17 (d, *J* = 6.66 Hz, 2H), 6.70 (dd, *J* = 5.8, 2.6 Hz, 1H), 6.76 (d, *J* = 2.3 Hz, 1H), 6.83 (d, *J* = 7.2 Hz, 1H), 8.20 (br d, *J* = 8.4 Hz, 1H), 7.23 7.31 (m, 2H), 8.14 (d, *J* = 7.2 Hz, 1H), 8.41 (d, *J* = 5.8 Hz, 1H). LC-MS *m*/*z* 443 [M + H]*, t_R = 2.70 min.
- 8-Chloro-3-cyclopropylmethyl-7-{4-[(2-ethylpyridin-4-yl)oxy]-3-fluororophenyl}[1,2,4]triazolo[4,3-a]-pyridine (17). Starting from 50a (0.26 g, 0.78 mmol) and 52d (0.293 g, 0.857 mmol) and following the procedure described for 8, compound 17 was obtained as a white solid (0.316 g, 96%). Mp > 300°C.

 ¹H NMR (500 MHz, CDCl₃) δ ppm 0.31 0.43 (m, 2H), 0.60 0.72 (m, 2H), 1.15 1.29 (m, 1H), 1.31 (t, J = 7.7 Hz, 3H), 2.82 (q, J = 7.6 Hz, 2H), 3.14 (d, J = 6.6 Hz, 2H), 6.72 (dd, J = 5.8, 2.3 Hz, 1H), 6.81 (d, J = 2.3 Hz, 1H), 6.91 (d, J = 6.9 Hz, 1H), 7.31 (t, J = 8.2 Hz, 1H), 7.35 7.42 (m, 1H), 7.45 (dd, J = 10.7, 2.0 Hz, 1H), 8.01 (d, J = 6.9 Hz, 1H), 8.44 (d, J = 5.8 Hz, 1H). LC–MS m/z 423 [M + H]⁺, t_p = 2.04 min.
- 8-Trifluoromethyl-3-cyclopropylmethyl-7-{4-[(2,6-dimethylpyridin-4-yl)oxy]-3-fluororophenyl}[1,2,4] triazolo[4,3-a]-pyridine (18). Starting from 49a (0.185 g, 0.67 mmol) and 52e (0.3 g, 0.874 mmol) and following the procedure described for 8, compound 18 was obtained as a white solid (0.100 g, 33%). Mp 232.5°C. ¹H NMR (500 MHz, CDCl₃) δ ppm 0.24 0.50 (m, 2H) 0.55 0.79 (m, 2H) 1.05 1.39 (m, 1H) 2.50 (s, 6H) 3.17 (d, *J*=6.70 Hz, 2H) 6.56 (s, 2H) 6.84 (d, *J*=7.17 Hz, 1H) 7.16 7.21 (m, 1H) 7.22 7.29 (m, 2H) 8.14 (d, *J*=7.17 Hz, 1 H). LC-MS *m*/z 457 [M + H]⁺, t_p = 2.94 min.
- 8-Chloro-3-cyclopropylmethyl-7-{4-[(2-cyclopropylpyridin-4-yl)oxy]-3-fluororophenyl}[1,2,4] triazolo[4,3-a]-pyridine (19). Starting from 50a (0.103 g, 0.310 mmol) and 52f (0.22 g, 0.310 mmol) and following the procedure described for 8, compound 19 was obtained as a white solid (0.06 g, 45%). Mp > 300°C. ¹H NMR (500 MHz, CDCl₃) δ ppm 0.38 (q, *J* = 5.11 Hz, 2H), 0.62 0.71 (m, 2H), 0.95 1.09 (m, 4H), 1.16 1.29 (m, 1H), 1.94 2.03 (m, 1H), 3.14 (d, *J* = 6.65 Hz, 2H), 6.66 (dd, *J* = 5.64, 2.46 Hz, 1H), 6.78 (d, *J* = 2.31 Hz, 1H), 6.90 (d, *J* = 6.94 Hz, 1H), 7.28 7.33 (m, 1H), 7.34 7.40 (m, 1H), 7.44 (dd, *J* = 10.69, 2.02 Hz, 1H), 8.00 (d, *J* = 6.94 Hz, 1H), 8.35 (d, *J* = 5.78 Hz, 1H). LC-MS *m*/*z* 435 [M + H]⁺, t_R = 4.51 min.
- 8-Trifluoromethyl-3-cyclopropylmethyl-7-{4-[(2-cyclopropylpyridin-4-yl)oxy]-3-fluororophenyl}[1,2,4] triazolo[4,3-a]-pyridine (20). Starting from 49a (0.2 g, 0.725 mmol) and 52f (0.283 g, 0.798 mmol) and following the procedure described for 8, compound 20 was obtained as a white solid (0.058 g, 17%). Mp 211.1°C. ¹H NMR (500 MHz, CDCl₃) δ ppm 0.32-0.45 (m, 2H), 0.53 0.75 (m, 2H), 0.96 1.03 (m, 2H), 1.02 1.08 (m, 2H), 1.16 1.30 (m, 1H), 1.91 2.03 (m, 1H), 3.16 (d, J = 6.7 Hz, 2H), 6.63 (dd, J = 5.8, 2.3 Hz, 1H), 6.75 (d, J = 2.3 Hz, 1H), 6.83 (d, J = 7.2 Hz, 1H), 7.15-7.22 (m, 1H), 7.22 7.31 (m, 2H), 8.15 (d, J = 6.9 Hz, 1H), 8.35 (d, J = 5.5 Hz, 1H). LC-MS m/z 469 [M + H] $^+$, t_g = 3.31 min.

- 8-Chloro-3-(2,2,2-trifluoroethyl-7-(4-[(2,6-dimethylpyridin-3-yl)oxy]-3-fluorophenyl}[1,2,4]triazolo[4,3-a]-pyridine (21). Starting from 56c (0.2 g, 0.55 mmol) and 52a (0.228 g, 0.664 mmol) and following the procedure described for 8, compound 21 was obtained as a white solid (0.032 g, 13%). Mp 164.5°C.

 ¹H NMR (500 MHz, CDCl₃) δ ppm 2.53 (s, 3H), 2.55 (s, 3H), 4.11 (q, J = 9.9 Hz, 2H), 6.93 (t, J = 8.3 Hz, 1H), 6.98 (d, J = 7.2 Hz, 1H), 7.02 (d, J = 8.3 Hz, 1H), 7.16 (d, J = 8.3 Hz, 1H), 7.23 7.28 (m, 1H), 7.42 (dd, J = 11.1, 2.1 Hz, 1H), 8.01 (d, J = 7.2 Hz, 1H). LC-MS m/z 451 [M + H]*, t_n = 3.24 min.
- 8-Chloro-3-(ethoxymethyl-7-{4-[(2,6-dimethylpyridin-3-yl)oxy]-3-fluorophenyl}[1,2,4]triazolo[4,3-a]-pyridine (22). Starting from 50b (0.4 g, 1.19 mmol) and 52a (0.488 g, 1.42 mmol) and following the procedure described for 8, compound 22 was obtained as a white solid (0.310 g, 61%). Mp 180.3°C.

 ¹H NMR (500 MHz, CDCl₃) δ ppm 1.23 (t, *J* = 6.94 Hz, 3H), 2.54 (s, 3 H), 2.55 (s, 3H), 3.58 (q, *J* = 6.94 Hz, 2H), 5.10 (s, 2H), 6.87 6.95 (m, 2H), 7.02 (d, *J* = 8.09 Hz, 1H), 7.16 (d, *J* = 8.09 Hz, 1H), 7.22 7.26 (m, 1H), 7.42 (dd, *J* = 11.27, 2.31 Hz, 1H), 8.25 (d, *J*=7.22 Hz, 1H). LC–MS *m/z* 427 [M + H]⁺, t_p = 2.77 min.
- 8-Trifluoromethyl-3-(ethoxymethyl-7-{4-[(2,6-dimethylpyridin-3-yl)oxy]-3-fluorophenyl}[1,2,4] triazolo[4,3-a]-pyridine (23). Starting from 49b (0.150 g, 0.536 mmol) and 52a (0.239 g, 0.697 mmol) and following the procedure described for 8, compound 23 was obtained as a white solid (0.150 g, 61%). Mp 142.2°C. ¹H NMR (500 MHz, CDCl₃) δ ppm 1.23 (t, *J*=7.08 Hz, 3H), 2.53 (s, 3H), 2.54 (s, 3H), 3.59 (q, *J* = 7.13 Hz, 2H), 5.12 (s, 2H), 6.82 (d, *J* = 7.22 Hz, 1H), 6.90 (t, *J* = 8.24 Hz, 1H), 7.01 (d, *J* = 8.38 Hz, 1H), 7.06 (d, *J* = 8.09 Hz, 1H), 7.14 (d, *J* = 8.38 Hz, 1H), 7.23 (dd, *J* = 10.69, 2.02 Hz, 1H), 8.40 (d, *J* = 6.94 Hz, 1H). LC-MS *m*/*z* 461 [M + H]*, t_p = 2.89 min.
- 8-Chloro-3-cyclopropylmethyl-7-[3-fluoro-4-(isopropylamino)-phenyl][1,2,4]triazolo[4,3-a]-pyridine (24). Starting from 50a (0.350 g, 1.049 mmol) and 52g (0.381 g, 1.36 mmol) and following the procedure described for 8, compound 24 was obtained as a white solid (0.097 g, 26%). Mp 196.4°C. ¹H NMR (500 MHz, CDCl₃) δ ppm 0.35 (q, *J* = 5.20 Hz, 2H), 0.60 0.67 (m, 2H), 1.15 1.26 (m, 1H), 1.29 (d, *J* = 6.36 Hz, 6H), 3.10 (d, *J* = 6.65 Hz, H), 3.72 (dq, *J* = 13.19, 6.49 Hz, 1H), 3.98 (br d, *J* = 5.20 Hz, 1H), 6.70 6.81 (m, 1H), 6.87 (d, *J* = 6.94 Hz, 1H), 7.17 7.31 (m, 2H) 7.91 (d, *J* = 7.22 Hz, 1H). LC-MS *m*/*z* 359 [M + H]*, t_p = 3.11 min.
- 8-Trifluoromethyl-3-cyclopropylmethyl-7-[3-fluoro-4-(isopropylamino)-phenyl][1,2,4]triazolo[4,3-a]-pyridine (25). Starting from 49a (0.350 g, 1.27 mmol) and 52g (0.461 g, 1.65 mmol) and following the procedure described for 8, compound 25 was obtained as a white solid (0.250 g, 50%). Mp 196.9°C. ¹H NMR (500 MHz, CDCl₃) δ ppm 0.28-0.42 (m, 2H), 0.57 0.71 (m, 2H), 1.12 1.26 (m, 1H), 1.29 (d, *J* = 6.4 Hz, 6H), 3.12 (d, *J* = 6.6 Hz, 2H), 3.64-3.77 (m, 1H), 3.96 (d, *J* = 4.9 Hz, 1H), 6.74 (t, *J* = 8.4 Hz, 1H), 6.80 (d, *J* = 7.2 Hz, 1H), 7.02 (d, *J* = 10.1 Hz, 2H), 8.04 (d, *J* = 6.9 Hz, 1H). LC-MS *m/z* 393 [M + H]*, t_R = 3.33 min.
- 8-Trifluoromethyl-3-cyclopropylmethyl-7-[3-chloro-4-(isopropylamino)-phenyl][1,2,4]triazolo[4,3-a]-pyridine (26). Starting from 49a (0.350 g, 1.27 mmol) and 52h (0.488 g, 1.65 mmol) and following the procedure described for 8, compound 26 was obtained as a white solid (0.250 g, 50%). Mp 230°C. 1 H NMR (500 MHz, CDCl₃) δ ppm 0.29 0.42 (m, 2H), 0.55 0.71 (m, 2H), 1.11 1.27 (m, 1H), 1.31 (d, J = 6.36 Hz, 6H), 3.13 (d, J = 6.65 Hz, 2H), 3.73 (dq, J = 13.11, 6.51 Hz, 1H), 4.38 (br d, J = 7.51 Hz, 1H), 6.71 (d, J = 8.67 Hz, 1H), 6.79 (d, J = 7.22 Hz, 1H), 7.16 (dd, J = 8.38, 1.44 Hz, 1H), 7.30 (d, J = 2.02 Hz, 1H), 8.03 (d, J = 6.94 Hz, 1H). LC-MS m/z 409 [M + H]*, t_R = 3.71 min.
- 8-Chloro-3-cyclopropylmethyl-7-[3-fluoro-4-(cyclopropylamino)-phenyl][1,2,4]triazolo[4,3-a]-pyridine (27). Starting from 50a (0.30 g, 0.9 mmol) and 52i (0.3 g, 1.08 mmol) and following the procedure described for 8, compound 27 was obtained as a white solid (0.147 g, 46%). ¹H NMR (500 MHz, CDCl₃) δ ppm 0.28 0.40 (m, 2H), 0.57 0.69 (m, 4H), 0.78 0.87 (m, 2H), 1.15 1.28 (m, 1H), 2.45 2.56 (m, 1H), 3.11 (d, *J* = 6.65 Hz, 2H), 4.60 (br s, 1H), 6.88 (d, *J* = 7.22 Hz, 1H), 7.13 7.20 (m, 1H), 7.21 7.31 (m, 2H), 7.92 (d, *J* = 6.94 Hz, 1H). LC-MS *m*/*z* 357 [M + H]*, t_p = 3.30 min.
- 8-Trifluoromethyl-3-cyclopropylmethyl-7-[3-fluoro-4-(cyclopropylamino)-phenyl][1,2,4]triazolo[4,3-a]-pyridine (28). Starting from 49a (0.20 g, 0.73 mmol) and 52i (0.221 g, 0.8 mmol) and following the procedure described for 8, compound 28 was obtained as a white solid (0.169 g, 60%). Mp. > 300°C.

 ¹H NMR (400 MHz, CDCl₃) δ ppm 0.28 0.43 (m, 2H), 0.51 0.72 (m, 4H), 0.75 0.91 (m, 2H), 1.12 1.31 (m, 1H), 2.50 (tt, *J* = 6.56, 3.27 Hz, 1H), 3.13 (d, *J* = 6.70 Hz, 2H), 4.58 (br s, 1H), 6.80 (d, *J* = 6.94 Hz, 1H), 6.98 7.09 (m, 2H), 7.10 7.18 (m, 1H), 8.05 (d, *J* = 7.17 Hz, 1H). LC-MS *m*/z 391 [M + H]*, t_P = 3.18 min.
- 8-Trifluoromethyl-3-cyclopropylmethyl-7-[3-chloro-4-(cyclopropylamino)-phenyl][1,2,4]triazolo[4,3-a]-pyridine (29). Starting from 49a (0.20 g, 0.73 mmol) and 52j (0.34 g, 0.8 mmol) and following the procedure described for 8, compound 29 was obtained as a white solid (0.109 g, 37%). ¹H NMR (400 MHz, CDCl₃) δ ppm 0.31 0.40 (m, 2H), 0.59 0.69 (m, 4H), 0.81 0.89 (m, 2H), 1.15 1.27 (m, 1H), 2.46 2.56 (m, 1H), 3.13 (d, *J* = 6.70 Hz, 2H), 4.93 (s, 1H), 6.80 (d, *J* = 7.17 Hz, 1H), 7.11 7.16 (m, 1H), 7.17 7.23 (m, 1H), 7.28 (d, *J* = 1.85 Hz, 1H), 8.05 (d, *J* = 7.17 Hz, 1H). LC-MS *m/z* 407 [M + H]⁺, t_R = 3.48 min.

- 8-Chloro-3-cyclopropylmethyl-7-[3-chloro-4-(cyclopropylamino)-phenyl][1,2,4]triazolo[4,3-a]-pyridine (30). Starting from 50a (0.30 g, 0.9 mmol) and 52j (0.32 g, 1.08 mmol) and following the procedure described for 8, compound 30 was obtained as a white solid (0.147 g, 46%). Mp > 300°C. ¹H NMR (500 MHz, CDCl₃) δ ppm 0.29 0.42 (m, 2H), 0.57 0.70 (m, 4H), 0.78 0.92 (m, 2H), 1.15 1.27 (m, 1H), 2.49 2.56 (m, 1H), 3.11 (d, *J* = 6.7 Hz, 2H), 4.60 (br s, 1H), 6.87 (d, *J* = 6.9 Hz, 1H), 7.18 (d, *J* = 8.3 Hz, 1H), 7.42 dd, *J* = 8.3, 2.1 Hz, 1H), 7.47 (d, *J* = 1.8 Hz, 1H), 7.92 (d, *J* = 7.2 Hz, 1H). LC-MS *m*/*z* 373 [M + H]*, t_p = 3.83 min.
- 8-Trifluoromethyl-3-cyclopropylmethyl-7-{4-[(2-methoxypyridin-5-yl)methoxy]-3-fluorophenyl} [1,2,4] triazolo[4,3-a]-pyridine (31). Starting from 49a (0.3 g, 1.088 mmol) and 52k (0.721 g, 1.306 mmol) and following the procedure described for 8, compound 31 was obtained as a white solid (0.198 g, 38%). Mp 148.5°C. ¹H NMR (400 MHz, CDCl₃) δ ppm 0.37 (q, *J* = 5.09 Hz, 2H), 0.56 0.74 (m, 2H), 1.09 1.32 (m, 1H), 3.14 (d, *J* = 6.70 Hz, 2H), 3.96 (s, 3H), 5.12 (s, 2H), 6.79 (dd, *J* = 13.87, 7.63 Hz, 2H), 7.00 7.19 (m, 3H), 7.71 (dd, *J* = 8.55, 2.54 Hz, 1H) 8.09 (d, *J* = 7.17 Hz, 1H), 8.24 (d, *J* = 2.31 Hz, 1H). LC-MS *m/z* 473 [M + H]⁺, t_p = 2.79 min.
- 8-Trifluoromethyl-3-cyclopropylmethyl-7-{4-[(2-methoxypyridin-5-yl)methoxy]- phenyl }[1,2,4] triazolo[4,3-a]-pyridine (32). Starting from 49a (0.315 g, 1.15 mmol) and 52l (0.430 g, 1.26 mmol) and following the procedure described for 8, compound 32 was obtained as a white solid (0.286 g, 60%). Mp 159.1°C. ¹H NMR (400 MHz, CDCl₃) δ ppm 0.29 0.45 (m, 2H), 0.55 0.72 (m, 2H), 1.10 1.33 (m, 1H), 3.14 (d, *J* = 6.70 Hz, 2H), 3.96 (s, 3H), 5.04 (s, 2H), 6.67 6.87 (m, 2H), 7.00 7.12 (m, 2H), 7.32 (d, *J* = 8.55 Hz, 2H), 7.70 (dd, *J* = 8.55, 2.31 Hz, 1H), 8.08 (d, *J* = 7.17 Hz, 1H), 8.25 (d, *J* = 2.31 Hz, 1H). LC-MS *m*/*z* 455 [M + H]*, t_p = 3.73 min.
- 8-Trifluoromethyl-3-cyclopropylmethyl-7-{4-[(2-methoxypyridin-5-yl)methylamino]-3-fluorophenyl} [1,2,4]triazolo[4,3-a]-pyridine (33). Starting from 49a (0.530 g, 1.92 mmol) and 52m (0.758 g, 2.11 mmol) and following the procedure described for 8, compound 33 was obtained as a white solid (0.460 g, 51%). Mp 160.4°C. ¹H NMR (400 MHz, CDCl₃) δ ppm 0.30 0.42 (m, 2H), 0.59 0.71 (m, 2H), 1.15 1.27 (m, 1H), 3.13 (d, J = 6.70 Hz, 2H), 3.95 (s, 3H), 4.36 (d, J = 4.86 Hz, 2H), 4.44 (br s, 1H), 6.69 6.83 (m, 3H), 6.95 7.12 (m, 2H), 7.62 (dd, J = 8.44, 2.43 Hz, 1H), 8.05 (d, J = 7.17 Hz, 1H), 8.19 (d, J = 2.54 Hz, 1H). LC-MS m/z 472 [M + H]*, t_R = 2.67 min.
- 8-Trifluoromethyl-3-cyclopropylmethyl-7-{4-[(2-methoxypyridin-5-yl)methylamino]-3-phenyl}[1,2,4] triazolo[4,3-a]-pyridine (34). Starting from 49a (0.150 g, 0.544 mmol) and 52n (0.204 g, 0.6 mmol) and following the procedure described for 8, compound 34 was obtained as a white solid (0.115 g, 46%). Mp 127.5°C. ¹H NMR (500 MHz, CDCl₃) δ ppm 0.29 0.42 (m, 2H), 0.60 0.68 (m, 2H), 1.17 1.24 (m, 1H), 3.12 (d, *J* = 6.94 Hz, 2H), 3.95 (s, 3H), 4.20 (br s, 1H), 4.32 (d, *J* = 4.91 Hz, 2H), 6.70 (d, *J* = 8.38 Hz, 2H), 6.76 (d, *J* = 8.38 Hz, 1H), 6.80 (d, *J* = 6.94 Hz, 1H), 7.21 (d, *J* = 8.67 Hz, 2H), 7.61 (dd, *J* = 8.53, 2.46 Hz, 1H), 8.03 (d, *J* = 7.22 Hz, 1H), 8.18 (d, *J* = 2.31 Hz, 1H). LC-MS *m*/*z* 454 [M + H]*, t_R = 2.05 min.
- 8-Chloro-3-cyclopropylmethyl-7-{4-[(2-methoxypyridin-5-yl)methylamino]-3-phenyl} [1,2,4] triazolo[4,3-a]-pyridine (35). Starting from 50a (0.150 g, 0.45 mmol) and 52n (0.168 g, 0.494 mmol) and following the procedure described for 8, compound 35 was obtained as a white solid (0.098 g, 51%). Mp 158.1°C. ¹H NMR (400 MHz, CDCl₃) δ ppm 0.30 0.40 (m, 2H), 0.57 0.70 (m, 2H), 1.13 1.39 (m, 1H), 3.10 (d, *J* = 6.70 Hz, 2H), 3.95 (s, 3H), 4.33 (s, 3H), 6.69 6.79 (m, 3H), 6.89 (d, *J* = 7.17 Hz, 1H), 7.38 7.46 (m, 2H), 7.62 (dd, *J* = 8.55, 2.54 Hz, 1H), 7.91 (d, *J* = 7.17 Hz, 1H), 8.19 (d, *J* = 2.08 Hz, 1H). LC-MS *m*/*z* 420 [M + H]*, t_p = 1.93 min.
- 8-Chloro-3-cyclopropylmethyl-7-[3-chloro-4-(tetrahydro-pyran-4-yloxy)-phenyl][1,2,4]triazolo[4,3-a]-pyridine (36). Starting from 50a (0.20 g, 0.6 mmol) and 52o (0.243 g, 0.72 mmol) and following the procedure described for 8, compound 36 was obtained as a white solid (0.160 g, 64%). Mp. 189.1°C.

 ¹H NMR (400 MHz, CDCl₃) δ ppm 0.30 0.43 (m, 2H), 0.56 0.73 (m, 2H), 1.15 1.30 (m, 1H), 1.92 (ddt, *J* = 17.05, 7.28, 3.55, 3.55 Hz, 2H), 2.02 2.17 (m, 2H), 3.12 (d, *J* = 6.70 Hz, 2H), 3.65 (ddd, *J* = 11.44, 7.40, 3.58 Hz, 2H), 4.66 (tt, *J* = 7.11, 3.64 Hz, 1H), 6.86 (d, *J* = 6.94 Hz, 1H), 7.06 (d, *J* = 8.55 Hz, 1H), 7.43 (dd, *J* = 8.55, 2.31 Hz, 1H), 7.58 (d, *J* = 2.31 Hz, 1H), 7.96 (d, *J* = 7.17 Hz, 1H). LC-MS *m*/*z* 418 [M + H]*, t_p = 3.25 min.
- 8-Trifluoromethyl-3-cyclopropylmethyl-7-[3-chloro-4-(tetrahydro-pyran-4-yloxy)-phenyl][1,2,4] triazolo[4,3-a]-pyridine (37). Starting from 49a (0.09 g, 0.33 mmol) and 52o (0.138 g, 0.41 mmol) and following the procedure described for 8, compound 37 was obtained as a white solid (0.083 g, 56%). Mp. 176.9°C. ¹H NMR (400 MHz, CDCl₃) δ ppm 0.30 0.43 (m, 2H), 0.58 0.73 (m, 2H), 1.16 1.28 (m, 1H), 1.86-1.97 (m, 2H), 2.02 2.12 (m, 2H), 3.14 (d, J = 6.70 Hz, H), 3.59-3.69 (m, 2H), 4-4.09 (m, 2H), 4.61-4.68 (m, 2H), 6.78 (d, J = 7.2 Hz, 1H), 7.02 (d, J = 8.6 Hz, 1H), 7.20 (dd, J = 8.6, 2.1 Hz, 1H), 7.41 (d, J = 2.1 Hz, 1H), 8.09 (d, J = 7.2 Hz, 1H). LC-MS m/z 452 [M + H]*, t_R = 3.33 min.

- 8-Chloro-3-cyclopropylmethyl-7-[3-chloro-4-(tetrahydro-pyran-4-ylamino)-phenyl][1,2,4]triazolo[4,3-a]-pyridine (38). Starting from 50a (0.20 g, 0.6 mmol) and 52p (0.242 g, 0.72 mmol) and following the procedure described for 8, compound 38 was obtained as a white solid (0.160 g, 64%). Mp. 221.3°C.

 ¹H NMR (500 MHz, CDCl₃) δ ppm 0.28 0.41 (m, 2H), 0.56 0.71 (m, 2H), 1.13 1.29 (m, 1H), 1.45 1.71 (m, 2H), 2.10 (br d, *J* = 13.29 Hz, 2H), 3.11 (d, *J* = 6.65 Hz, 2H), 3.52 3.60 (m, 2H), 3.62 (br dd, *J* = 6.94, 3.18 Hz, 1H), 4.05 (dt, *J* = 11.78, 3.65 Hz, 2H), 4.49 (br d, *J* = 7.80 Hz, 1H), 6.78 (d, *J* = 8.38 Hz, 1H), 6.86 (d, *J* = 7.22 Hz, 1H), 7.39 (dd, *J* = 8.53, 2.17 Hz, 1H), 7.51 (d, *J* = 2.31 Hz, 1H), 7.92 (d, *J* = 7.22 Hz, 1H). LC-MS *m*/*z* 417 [M + H]*, t_z = 4.08 min.
- 8-Trifluoromethyl-3-cyclopropylmethyl-7-[3-chloro-4-(tetrahydro-pyran-4-ylamino)-phenyl][1,2,4] triazolo[4,3-a]-pyridine (39). Starting from 49a (0.07 g, 0.25 mmol) and 52p (0.107 g, 0.32 mmol) and following the procedure described for 8, compound 39 was obtained as a white solid (0.045 g, 39%). Mp. 198.4°C. ¹H NMR (400 MHz, CDCl₃) δ ppm 0.31 0.42 (m, 2H), 0.58 0.71 (m, 2H), 1.16 1.27 (m, 1H), 1.55 1.68 (m, 2H), 2.09 (br d, *J* = 12.7 Hz, 2H), 3.13 (d, *J* = 6.7 Hz, 2H), 3.56 (td, *J* = 11.8, 2.3 Hz, 1H), 3.56-3.67 (m, 1H), 4.05 (dt, *J* = 11.7, 3.7 Hz, 2H), 4.47 (d, *J* = 7.6 Hz, 1H), 6.74 (d, *J* = 8.6 Hz, 1H), 6.78 (d, *J* = 7.2 Hz, 1H), 7.16 (dd, *J* = 8.3, 1.8 Hz, 1H), 7.32 (d, *J* = 2.1 Hz, 1H), 8.05 (d, *J* = 7.2 Hz, 1H). LC-MS *m/z* 451 [M + H]*, t₀ = 3.29 min.
- 8-Trifluoromethyl-3-cyclopropylmethyl-7-[3-chloro-4-(tetrahydro-pyran-4-ylaminomethyl)-phenyl] [1,2,4]triazolo[4,3-a]-pyridine (40). Starting from 49a (0.2 g, 0.73 mmol) and 52q (0.306 g, 0.87 mmol) and following the procedure described for 8, compound 40 was obtained as a white solid (0.060 g, 18%). ¹H NMR (400 MHz, CDCl₃) δ ppm 0.37 (q, *J* = 5.09 Hz, 2H), 0.59 0.74 (m, 2H), 1.10 1.32 (m, 2H), 1.41 1.73 (m, 2H), 1.92 (br dd, *J* = 12.60, 1.73 Hz, 2H), 2.69 2.86 (m, 1H), 3.15 (d, *J* = 6.70 Hz, 2H), 3.34 3.49 (m, 2H), 3.97 4.01 (m, 3H), 4.01 4.04 (m, 1H), 6.76 (d, *J* = 7.17 Hz, 1H), 7.22 7.28 (m, 1H), 7.37 (d, *J* = 1.62 Hz, 1H), 7.56 (d, *J* = 7.86 Hz, 1H), 8.10 (d, *J* = 7.17 Hz, 1H). LC-MS *m/z* 465 [M + H]*, t_p = 2.09 min.
- Trans-8-Chloro-3-cyclopropylmethyl-7-[3-chloro-4-(4-hydroxy-cyclohexylamino)-phenyl][1,2,4] triazolo[4,3-a]-pyridine (41). Starting from 50a (0.13 g, 0.388 mmol) and 52r (0.15 g, 0.43 mmol) and following the procedure described for 8, compound 41 was obtained as a white solid (0.087 g, 52%). Mp 270.9°C. ¹H NMR (400 MHz, CDCl₃) δ ppm 0.29 0.42 (m, 2H), 0.56 0.71 (m, 2H), 1.17 1.25 (m, 1H), 1.47 (br s, 1H), 1.73 1.8 (m, 4H), 1.80-1.91 (m, 4H), 3.11 (d, J=6.7 Hz, 2H), 3.46 3.57 (m, 1H), 3.98 (br s, 1H), 4.60 (br d, J=7.6 Hz, 1H), 6.76 (d, J=8.8 Hz, 1H), 6.87 (d, J=7.2 Hz, 1H), 7.39 (dd, J=8.3, 2.3 Hz, 1H), 7.49 (d, J=2.1 Hz, 1H), 7.91 (d, J=7.2 Hz, 1H). LC-MS m/z 431 [M + H]*, t_R = 3.49 min.
- *Trans*-8-Trifluoromethyl-3-cyclopropylmethyl-7-[3-chloro-4-(4-hydroxy-cyclohexylamino)-phenyll [1,2,4]triazolo[4,3-a]-pyridine (42). Starting from 49a (0.3 g, 1.088 mmol) and 52r (0.459 g, 1.306 mmol) and following the procedure described for 8, compound 42 was obtained as a white solid (0.209 g, 41%). Mp. 290.7°C. ¹H NMR (400 MHz, CDCl₃) δ ppm 0.3 0.43 (m, 2H), 0.58 0.71 (m, 2H), 1.16 1.25 (m, 1H), 1.29-1.42 (m, 2H), 1.42 1.53 (m, 3H), 2.03-2.12 (m, 2H), 2.20 (br d, J = 12.0 Hz, 2H), 3.13 (d, J=6.7 Hz, 2H), 3.32 3.43 (m, 1H), 3.70-3.80 (m, 1H), 4.39 (d, J = 7.6 Hz, 1H), 6.72 (d, J = 8.6 Hz, 1H), 6.79 (d, J = 7.2 Hz, 1H), 7.16 (dd, J = 8.6, 2.1 Hz, 1H), 7.30 (d, J = 2.1 Hz, 1H), 8.04 (d, J = 7.2 Hz, 1H). LC-MS m/z 465 [M + H]*, t_R = 2.50 min.
- *Cis*-8-Chloro-3-cyclopropylmethyl-7-[3-chloro-4-(4-hydroxy-cyclohexylamino)-phenyl][1,2,4] triazolo[4,3-a]-pyridine (43). Starting from 50a (0.13 g, 0.388 mmol) and 52s (0.15 g, 0.43 mmol) and following the procedure described for 8, compound 43 was obtained as a white solid (0.060 g, 36%). Mp. 273.7°C. ¹H NMR (400 MHz, CDCl₃) δ ppm 0.27 0.43 (m, 2H) 0.57 0.70 (m, 2H), 1.02 1.32 (m, 2H), 1.68 1.98 (m, 8H), 3.11 (d, J = 6.70 Hz, 2H), 3.44 3.62 (m, 1H), 3.98 (br s, 1H), 4.60 (br d, J = 7.63 Hz, 1H), 6.76 (d, J = 8.79 Hz, 1H), 6.87 (d, J = 7.17 Hz, 1H), 7.39 (dd, J = 8.44, 2.20 Hz, 1H), 7.49 (d, J = 2.08 Hz, 1H), 7.91 (d, J = 7.17 Hz, 1H). LC-MS m/z 431 [M + H]*, $t_p = 3.08$ min.
- *Cis*-8-Trifluoromethyl-3-cyclopropylmethyl-7-[3-chloro-4-(4-hydroxy-4-cyclopropyl-cyclohexylamino)-phenyl][1,2,4]triazolo[4,3-a]-pyridine (44). Starting from 49a (0.143 g, 0.52 mmol) and 52t (0.235 g, 0.6 mmol) and following the procedure described for 8, compound 44 was obtained as a white solid (0.047 g, 18%). Mp > 300°C. ¹H NMR (500 MHz, CDCl₃) δ ppm 0.04 0.16 (m, 2H), 0.18 0.33 (m, 5H), 0.34 0.43 (m, 2H), 0.60 (tt, *J* = 8.31, 5.56 Hz, 1H), 0.80 1.00 (m, 1H), 1.11 1.25 (m, 2H), 1.31 1.56 (m, 4H), 1.63 1.79 (m, 2H), 2.49 (d, *J* = 6.65 Hz, 2H), 2.97 (tdt, *J* = 11.13, 11.13, 7.37, 3.97, 3.97 Hz, 1H), 4.45 (d, *J* = 7.51 Hz, 1H), 5.95 (d, *J* = 7.22 Hz, 1H), 6.53 (d, *J* = 8.67 Hz, 1H), 6.73 (d, *J* = 7.22 Hz, 1H), 7.16 (s, 1H) 7.28 (d, *J* = 2.02 Hz, 1H). LC-MS *m*/*z* 465 [M + H]*, t_n = 3.49 min.
- *Trans*-8-Chloro-3-(2,2,2-trifluoroethyl)-7-[3-chloro-4-(4-hydroxy-cyclohexylamino)-phenyl][1,2,4] triazolo[4,3-a]-pyridine (45). Starting from 56c (0.11 g, 0.304 mmol) and 52r (0.128 g, 0.365 mmol) and following the procedure described for 8, compound 45 was obtained as a white solid (0.054 g, 39%). Mp > 300°C. 1 H NMR (400 MHz, CDCl₃) δ ppm 1.28 1.52 (m, 5H), 2.08 (br d, J = 10.63 Hz, 2H), 2.20 (br d, J = 12.02 Hz, 2H), 3.26 3.46 (m, 1H), 3.62 3.85 (m, 1H), 4.08 (q, J = 9.71 Hz, 2H), 4.44 (d, J =

- 7.63 Hz, 1H), 6.77 (d, J = 8.55 Hz, 1H), 6.97 (d, J = 7.17 Hz, 1H), 7.39 (dd, J = 8.55, 2.08 Hz, 1H), 7.50 (d, J = 2.08 Hz, 1H), 7.94 (d, J = 7.17 Hz, 1H). LC-MS m/z 459 [M + H]*, $t_p = 3.23$ min.
- *Trans*-8-Trifluoromethyl-3-cyclopropylmethyl-7-[3-chloro-4-(4-hydroxy-cyclohexyloxy)-phenyl][1,2,4] triazolo[4,3-a]-pyridine (46). Starting from 49a (0.119 g, 0.432 mmol) and 52u (0.183g, 0.518 mmol) and following the procedure described for 8, compound 46 was obtained as a white solid (0.022 g, 27%). ¹H NMR (400 MHz, CDCl₃) δ ppm 0.31 0.41 (m, 2H), 0.61 0.71 (m, 2H), 1.09 1.32 (m, 2H), 1.42 1.56 (m, 2H), 1.67 1.80 (m, 2H), 2.05 2.23 (m, 4H), 3.14 (d, *J* = 6.70 Hz, 2H), 3.83 3.96 (m, 1H), 4.36 4.49 (m, 1H), 6.78 (d, *J* = 7.17 Hz, 1H), 7.02 (d, *J* = 8.79 Hz, 1H), 7.20 (dd, *J* = 8.44, 2.20 Hz, 1H), 7.39 (d, *J* = 2.31 Hz, 1H), 8.09 (d, *J* = 7.17 Hz, 1H). LC-MS *m/z* 466 [M + H]*, t_p = 2.96 min.
- Trans-8-Chloro-3-(2,2,2-trifluoroethyl)-7-[3-chloro-4-(4-hydroxy-cyclohexyloxy)-phenyl][1,2,4] triazolo[4,3-a]-pyridine (47). Starting from 56c (0.190 g, 0.526 mmol) and 52u (0.222 g, 0.631 mmol) and following the procedure described for 8, compound 47 was obtained as a white solid (0.065 g, 27%). Mp >300°C. ¹H NMR (500 MHz, CDCl₃) δ ppm 1.42 (d, *J* = 3.76 Hz, 1H), 1.46 1.55 (m, 2H), 1.68 1.79 (m, 2H), 2.10 (td, *J* = 7.73, 3.61 Hz, 2H), 2.18 (td, *J* = 7.66, 3.47 Hz, 2H), 3.91 (td, *J* = 8.09, 4.05 Hz, 1H), 4.10 (q, *J* = 9.73 Hz, 2H), 4.46 (tt, *J* = 8.06, 3.79 Hz, 1H), 6.97 (d, *J* = 7.22 Hz, 1H), 7.08 (d, *J* = 8.38 Hz, 1H), 7.42 (dd, *J* = 8.53, 2.17 Hz, 1H), 7.57 (d, *J* = 2.31 Hz, 1H), 7.98 (d, *J*=7.22 Hz, 1H). LC-MS *m*/z 460 [M + H]*, t_p = 3.23 min.
- Cis-8-Chloro-3-(2,2,2-trifluoroethyl)-7-[3-chloro-4-(4-hydroxy-cyclohexyloxy)-phenyl][1,2,4] triazolo[4,3-a]-pyridine (48). Starting from 56c (0.150 g, 0.415 mmol) and 52v (0.176g, 0.498 mmol) and following the procedure described for 8, compound 48 was obtained as a white solid (0.044 g, 23%). Mp 196.7°C. ¹H NMR (400 MHz, CDCl₃) δ ppm 1.39 1.48 (m, 1H), 1.66 1.93 (m, 6H), 2.06 2.21 (m, 2H), 3.81 (tq, *J* = 8.44, 4.24 Hz, 1H), 4.10 (q, *J* = 9.71 Hz, 2H), 4.56 (tt, *J* = 5.20, 2.77 Hz, 1H), 6.98 (d, *J* = 7.17 Hz, 1H), 7.06 (d, *J* = 8.55 Hz, 1H), 7.43 (dd, *J* = 8.55, 2.31 Hz, 1H), 7.57 (d, *J* = 2.31 Hz, 1H), 7.99 (d, *J* = 7.17 Hz, 1H). LC-MS *m*/*z* 460 [M + H]*, t_n = 3.14 min.
- 8-Trifluoromethyl-3-(ethoxymethyl)-7-[3-chloro-1,2,4-triazolo[4,3-a]-pyridine (49b). Mp 104°C. ¹H NMR (400 MHz, CDCl₃) δ ppm ¹H NMR (500 MHz, CHLOROFORM-d) δ ppm 1.22 (t, J=6.94 Hz, 3 H) 3.57 (q, J=6.94 Hz, 2 H) 5.08 (s, 2 H) 6.95 (d, J=7.22 Hz, 1 H) 8.35 (d, J=7.51 Hz, 1 H). LC-MS *m/z* 280 [M + H]⁺, t_p = 1.32 min.

Biology

Membrane preparation

CHO-K1 cells stably expressing the wildtype hmGlu $_2$ receptor (CHO-K1_hmGlu $_2$) were grown in DMEM medium supplemented with 10% (v/v) fetal calf serum, 200 IU/mL penicillin, 200 µg/mL streptomycin, 30.5 µg/mL L proline and 400 µg/mL G418 at 37°C and 5% CO $_2$. Sodium butyrate (final concentration 5 mM) was added to the plates when cells growth reached 70% confluency. ⁶³ 24 hours later, cells were detached from the plates by scraping into 5 ml of PBS and centrifuged for 5 min at 1500 rpm. Pellets were resuspended into ice-cold Tris buffer (50 mM Tris-HCl pH 7.4) and homogenized using an Ultra Turrax homogenizer (IKA Werke GmbH & Co.KG, Staufen, Germany). An Optima LE 80 K ultracentrifuge (Beckman Coulter, Fullerton, CA) at 31,000 rpm was used for separation of membranes and the cytosolic fraction at 4°C for 20 min. Pellets were resuspended in 10 ml Tris buffer and the centrifugation and homogenization steps were repeated. Remaining pellets were suspended into assay buffer (50 mM Tris-HCl pH 7.4, 2 mM CaCl $_2$, 10 mM MgCl $_2$) and the homogenization step was repeated. Aliquots were stored at -80°C. BCA protein determination was used to determine the membrane protein concentrations.

[35S]GTPyS Binding Assay

[35S]GTPyS binding experiments were performed as previously described.12

Radioligand Binding Assays

After thawing, membranes were homogenized by an Ultra Turrax homogenizer. 4 (10 μ M) was used to determine nonspecific binding. DMSO concentrations were $\leq 0.25\%$. For all experiments, radioligand concentrations were such that <10% of the amount added was receptor-bound to avoid ligand depletion.

For displacement assays, membrane protein aliquots (30 µg) were incubated with 6 nM [³H]-7 and 10 concentrations of competing ligand diluted by an HP D300 digital dispenser (Tecan, Giessen, The Netherlands) in assay buffer to a total volume of 100 µl. After 60 minutes at 15°C, incubation was terminated by rapid filtration over GF/C filterplates (PerkinElmer, Groningen, The Netherlands) on a PerkinElmer filtermate harvester. Filterplates were washed 10 times with ice-cold wash buffer (50 mM Tris-HCl pH 7.4) and filter-bound radioactivity was determined in a Microbeta 2450² microplate counter (PerkinElmer).

For association, dissociation and competition association experiments a scintillation proximity assay (SPA) was developed and used. Membrane protein (20 μ g) and pre-wetted wheat-germ agglutinin coated SPA beads (0.2 mg; RPNQ0001, PerkinElmer) were pre-coupled in assay buffer while gently shaking at room temperature for 30 minutes. Then, this membrane bead mixture was added to an Isoplate-96 (PerkinElmer) together with 6 nM [3 H]-7 and competing ligand in case of competition association. After addition, the plate was rapidly placed in a Microbeta 2450 2 microplate counter. Plates were recorded for 120 minutes measuring every 30 seconds at ambient temperature of 28°C. Binding values were determined in corrected counts per minute (CCPM). For dissociation assays, radioligand dissociation was initiated after 60 minutes of incubation by addition of 5 μ l 4 (final concentration: 10 μ M). Subsequently, plates were recorded for 120 minutes being measuring every 30 seconds.

Label-free whole-cell assays

Label-free whole-cell assays were performed using the xCELLigence real-time cell analyzer (RTCA DP) system as described previously 58,64 . Baseline impedance was measured using 45 μ l culture medium (as described under membrane preparation) per well in 16 well E-plates (Westburg, Leusden, The Netherlands). 40,000 cells per well were added in a volume of 50 μ l. After resting for 30 minutes at room temperature, E-plates were placed in the recording station within a humidified 37°C, 5% CO $_2$ incubator. Impedance (represented in the arbitrary unit Cell Index) was measured every 15 minutes overnight. After 18 hours, cells were stimulated with the indicated concentration of compound. Impedance was measured every 15 seconds for 20 minutes, then 5 minute intervals were used for the next 40 minutes, followed by 15 minute intervals thereafter. For washing experiments, cells were stimulated with an EC $_{80}$ equivalent concentration of compound in a volume of 5 μ l. Wells were washed after 5 minutes

by aspiration of the medium, addition of $100 \mu l$ fresh medium, which was subsequently aspirated and replaced by another $100 \mu l$ fresh medium. This washing step was chosen such that it was just before the maximum Cell Index level. In control wells, medium was pipetted up and down in order to induce similar mechanical cell stress.

Data Analysis

Data analyses were performed using Prism 6.04 (GraphPad software, San Diego, CA, USA). pIC_{50} values were acquired using non-linear regression curve fitting into a sigmoidal concentration-response curve using the equation: Y=Bottom + (Top-Bottom)/(1+10^(X-LogIC50)). pK_i values were acquired from pIC_{50} values using the Cheng-Prusoff equation. ⁶⁵ Dissociation rate constants k_{off} were determined using an exponential decay analysis of radioligand binding. Association rate constants k_{on} were determined using the equation $k_{on} = (k_{obs} - k_{off})/[L]$, in which L is the concentration of radioligand used for association experiments and k_{obs} was determined using exponential association analysis.

Association and dissociation rate constants for unlabelled mGlu₂ PAMs were determined by nonlinear regression analysis of competition association data as described by Motulsky and Mahan.⁴⁰

$$\begin{split} K_{A} &= k_{1}[L] \cdot 10^{-9} + k_{2} \\ K_{B} &= k_{3}[I] \cdot 10^{-9} + k_{4} \\ S &= \sqrt{(K_{A} - K_{B})^{2} + 4 \cdot k_{1} \cdot k_{3} \cdot L \cdot I \cdot 10^{-18}} \\ K_{F} &= 0.5(K_{A} + K_{B} + S) \\ K_{S} &= 0.5(K_{A} + K_{B} - S) \\ Q &= \frac{B_{\max} \cdot k_{1} \cdot L \cdot 10^{-9}}{K_{F} - K_{S}} \\ Y &= Q \cdot (\frac{k_{4} \cdot (K_{F} - K_{S})}{K_{F} \cdot K_{S}} + \frac{k_{4} - K_{F}}{K_{F}} e^{(-K_{F} \cdot X)} - \frac{k_{4} - K_{S}}{K_{S}} e^{(-K_{S} \cdot X)}) \end{split}$$

Experimental data are reported as k_{on} and k_{off} and the corresponding conversion of k_{off} to residence time (RT) is performed to be consistent with current state of the art.²⁴

Data shown are the mean \pm SEM of at least three individual experiments performed in duplicate unless stated otherwise. Statistical analysis was performed if indicated, using a two-tailed unpaired Student's t-test. Observed differences with p-values <0.05 were considered statistically significant. clogP values were calculated using ChemDraw Professional v15.0.0.106 (PerkinElmer).

REFERENCES

- 1. Kew JNC, Kemp JA. Psychopharmacology (Berl). 2005; 179: 4–29.
- Niswender CM, Conn PJ. Annu Rev Pharmacol Toxicol. 2010; 50: 295–322.
- Muto T, Tsuchiya D, Morikawa K, Jingami H. Proc Natl Acad Sci U S A. 2007; 104: 3759– 64
- Nicoletti F, Bockaert J, Collingridge GL, Conn PJ, Ferraguti F, Schoepp DD, Wroblewski JT, Pin JP. Neuropharmacology. 2011; 60: 1017–41.
- Dunayevich E, Erickson J, Levine L, Landbloom R, Schoepp DD, Tollefson GD. Neuropsychopharmacology. 2008; 33: 1603–10.
- Patil ST, Zhang L, Martenyi F, Lowe SL, Jackson KA, Andreev B V, Avedisova AS, Bardenstein LM, Gurovich IY, Morozova MA, Mosolov SN, Neznanov NG, Reznik AM, Smulevich AB, Tochilov VA, Johnson BG, Monn JA, Schoepp DD. Nat Med. 2007; 13: 1102–7.
- 7. Keov P, Sexton PM, Christopoulos A. *Neuropharmacology*. **2011**; 60: 24–35.
- 8. Trabanco AA, Cid JM. Expert Opin Ther Pat. **2013**; 23: 629–47.
- Johnson MP, Baez M, Jagdmann GE, Britton TC, Large TH, Callagaro DO, Tizzano JP, Monn JA, Schoepp DD. J Med Chem. 2003; 46: 3189–92.
- Galici R, Jones CK, Hemstapat K, Nong Y, Echemendia NG, Williams LC, de Paulis T, Conn PJ. J Pharmacol Exp Ther. 2006; 318: 173–85.
- 11. Fell MJ, Witkin JM, Falcone JF, Katner JS, Perry KW, Hart J, Rorick-Kehn L, Overshiner CD, Rasmussen K, Chaney SF, Benvenga MJ, Li X, Marlow DL, Thompson LK, Luecke SK, Wafford KA, Seidel WF, Edgar DM, Quets AT, Felder CC, Wang X, Heinz BA, Nikolayev A, Kuo M-S, Mayhugh D, Khilevich A, Zhang D, Ebert PJ, Eckstein JA, Ackermann BL, Swanson SP, Catlow JT, Dean RA, Jackson K, Tauscher-Wisniewski

- S, Marek GJ, Schkeryantz JM, Svensson KA. *J Pharmacol Exp Ther*. **2011**; 336: 165–177.
- Lavreysen H, Langlois X, Ahnaou A, Drinkenburg W, te Riele P, Biesmans I, Van der Linden I, Peeters L, Megens A, Wintmolders C, Cid JM, Trabanco AA, Andrés JI, Dautzenberg FM, Lütjens R, Macdonald G, Atack JR. J Pharmacol Exp Ther. 2013; 346: 514–27.
- 13. Cook D, Brown D, Alexander R, March R, Morgan P, Satterthwaite G, Pangalos MN. *Nat Rev Drug Discov.* **2014**; 13: 419–31.
- Homepage: http://clinicaltrials.gov. The Effects AZD8529 on Cognition and Negative Symptoms in Schizophrenics: https:// clinicaltrials.gov/show/NCT00986531 (accessed May 1, 2018).
- 15. Homepage: http://clinicaltrials.gov. The Study of AZD8529 for Smoking Cessation in Female Smokers: https://www.clinicaltrials.gov/ct2/show/NCT02401022?term=AZD8529&rank=1 (accessed May 1, 2018).
- Cid JM, Tresadern G, Duvey G, Lütjens R, Finn T, Rocher J, Poli S, Vega JA, de Lucas AI, Matesanz E, Linares ML, Andrés JI, Alcazar J, Alonso JM, Macdonald GJ, Oehlrich D, Lavreysen H, Ahnaou A, Drinkenburg W, Mackie C, Pype S, Gallacher D, Trabanco AA. J Med Chem. 2014; 57: 6495– 512.
- 17. Lavreysen H, Ahnaou A, Drinkenburg W, Langlois X, Mackie C, Pype S, Lütjens R, Le Poul E, Trabanco AA, Nuñez JMC. *Pharmacol Res Perspect.* **2015**; 3: e00096.
- 18. Lavreysen H, Langlois X, Ver Donck L, Cid Nuñez JM, Pype S, Lütjens R, Megens A. *Pharmacol Res Perspect.* **2015**; 3: e00097.
- Salih H, Anghelescu I, Kezic I, Sinha V, Hoeben E, Van Nueten L, De Smedt H, De Boer P. J Psychopharmacol. 2015; 29: 414–425.
- 20. Kent JM, Daly E, Kezic I, Lane R, Lim P, De Smedt H, De Boer P, Van Nueten L, Drevets

- WC, Ceusters M. *Prog Neuro-Psychopharma-cology Biol Psychiatry*. **2016**; 67: 66–73.
- http://www.addextherapeutics.com/ investors/press-releases/news-details/ article/addex-reports-top-linedata-froma-successful-phase-2a-clinical-study-withadx71149-inschizophrenia/ (accessed July 28, 2016).
- 22. http://clinicaltrials.gov/show/ NCT01582815 (accessed May 1, 2018).
- 23. Swinney DC. Curr Opin Drug Discov Devel. 2009; 12: 31–9.
- Copeland RA. Nat Rev Drug Discov. 2016;
 15: 87–95.
- Guo D, Heitman LH, IJzerman AP. ChemMedChem. 2015: 10: 1793–1796.
- Swinney DC, Haubrich BA, Liefde I Van, Vauquelin G. Curr Top Med Chem. 2015; 15: 2504–22.
- Guo D, Heitman LH, IJzerman AP. Chem Rev. 2016; 117: DOI: 10.1021/acs.chemrev.6b00025.
- 28. Guo D, Hillger JM, IJzerman AP, Heitman LH. *Med Res Rev.* **2014**; 34: 856–92.
- Dowling MR, Charlton SJ. Br J Pharmacol. 2006; 148: 927–37.
- Tresadern G, Bartolome JM, Macdonald GJ, Langlois X. Bioorg Med Chem. 2011; 19: 2231–41.
- 31. Kapur S, Seeman P. *Am J Psychiatry*. **2001**; 158: 360–369.
- 32. Yin N, Pei J, Lai L. *Mol Biosyst.* **2013**; 9: 1381–9.
- 33. Vauquelin G. *Br J Pharmacol.* **2016**; 173: 2319–2334.
- 34. Schoop A, Dey F. *Drug Discov Today Technol.* **2015**; 17: 9–15.
- 35. Cid JM, Tresadern G, Vega JA, de Lucas AI, Matesanz E, Iturrino L, Linares ML, Garcia A, Andrés JI, Macdonald GJ, Oehlrich D, Lavreysen H, Megens A, Ahnaou A, Drinkenburg W, Mackie C, Pype S, Gallacher D,

- Trabanco AA. J Med Chem. 2012; 55: 8770–89.
- Tresadern G, Cid J-MM, Trabanco AA. J Mol Graph Model. 2014; 53: 82–91.
- Cid-Nuñez, J. M., De Lucas Olivares, A. I., Trabanco-Suarez, A. A., MacDonald, G. J. 2010.
- Cid JM, Duvey G, Tresadern G, Nhem V, Furnari R, Cluzeau P, Vega JA, de Lucas AI, Matesanz E, Alonso JM, Linares ML, Andrés JI, Poli SM, Lutjens R, Himogai H, Rocher J, Macdonald GJ, Oehlrich D, Lavreysen H, Ahnaou A, Drinkenburg W, Mackie C, Trabanco AA. J Med Chem. 2012; 55: 2388–2405.
- 39. Doornbos MLJ, Pérez-Benito L, Tresadern G, Mulder-Krieger T, Biesmans I, Trabanco AA, Cid JM, Lavreysen H, IJzerman AP, Heitman LH. *Br J Pharmacol.* **2016**; 173: 588–600.
- 40. Motulsky HJ, Mahan LC. *Mol Pharmacol*. **1984**; 25: 1–9.
- 41. Xia L, de Vries H, IJzerman AP, Heitman LH. *Purinergic Signal*. **2016**; 12: 115–126.
- Farinha A, Lavreysen H, Peeters L, Russo B, Masure S, Trabanco AA, Cid J, Tresadern G. Br J Pharmacol. 2015; 172: 2383–96.
- Pérez-Benito L, Doornbos MLJ, Cordomí A, Peeters L, Lavreysen H, Pardo L, Tresadern G. Structure. 2017; 25: 1–10.
- 44. Lovering F, Bikker J, Humblet C. J Med Chem. 2009; 52: 6752–6756.
- Wacker D, Wang S, McCorvy JD, Betz RM, Venkatakrishnan AJ, Levit A, Lansu K, Schools ZL, Che T, Nichols DE, Shoichet BK, Dror RO, Roth BL. Cell. 2017; 168: 377–389.e12.
- 46. Sykes DA, Dowling MR, Charlton SJ. *Mol Pharmacol.* **2009**; 76: 543–51.
- 47. Guo D, Mulder-Krieger T, IJzerman AP, Heitman LH. Br J Pharmacol. 2012; 166: 1846–1859.
- 48. Deyrup MD, Nowicki ST, Richards NGJ, Otero DH, Harrison JK, Baker SP. *Naunyn*

- Schmiedebergs Arch Pharmacol. **1999**; 359: 168–77.
- 49. Mould R, Brown J, Marshall FH, Langmead CJ. *Br J Pharmacol.* **2014**; 171: 351–63.
- 50. Sykes D a, Charlton SJ. *Br J Pharmacol.* **2012**; 165: 2672–83.
- 51. Yu Z, Van Veldhoven JPD, Louvel J, 'T Hart IME, Rook MB, Van Der Heyden MAG, Heitman LH, IJzerman AP. *J Med Chem.* **2015**; 58: 5916–5929.
- Yu Z, IJzerman AP, Heitman LH. Br J Pharmacol. 2015; 172: 940–955.
- 53. de Witte WEA, Danhof M, van der Graaf PH, de Lange ECM. *Trends Pharmacol Sci.* **2016**; 37: 831–842.
- Vauquelin G, Charlton SJ. Br J Pharmacol. 2010; 161: 488–508.
- Vauquelin G. Expert Opin Drug Discov. 2015;
 10: 1085–1098.
- 56. Vauquelin G. *Br J Clin Pharmacol.* **2016**; 82: 673–682.
- 57. Perry DC, Mullis KB, Øie S, Sadée W. *Brain Res.* **1980**; 199: 49–61.
- Yu N, Atienza JM, Bernard J, Blanc S, Zhu J, Wang X, Xu X, Abassi Y. Anal Chem. 2006; 78: 35–43.
- Hillger JM, Diehl C, van Spronsen E, Boomsma DI, Slagboom PE, Heitman LH, IJzerman AP. Biochem Pharmacol. 2016; 115: 114–122.
- Xi B, Yu N, Wang X, Xu X, Abassi YA. Biotechnol J. 2008; 3: 484–495.
- Ahnaou A, Dautzenberg FM, Geys H, Imogai H, Gibelin A, Moechars D, Steckler T, Drinkenburg WHIM. Eur J Pharmacol. 2009; 603: 62–72.
- Ahnaou A, De Boer P, Lavreysen H, Huysmans H, Sinha V, Raeymaekers L, Van De Casteele T, Cid JM, Van Nueten L, MacDonald GJ, Kemp JA, Drinkenburg WHIM. Neuropharmacology. 2016; 103: 290–305.
- 63. Cuisset L, Tichonicky L, Jaffray P, Delpech M. *J Biol Chem.* **1997**; 272: 24148–24153.

- Hillger JM, Schoop J, Boomsma DI, Eline Slagboom P, IJzerman AP, Heitman LH. Biosens Bioelectron. 2015; 74: 233–242.
- 65. Cheng Y, Prusoff WH. *Biochem Pharmacol*. **1973**; 22: 3099–108.

SUPPORTING FIGURES AND TABLE

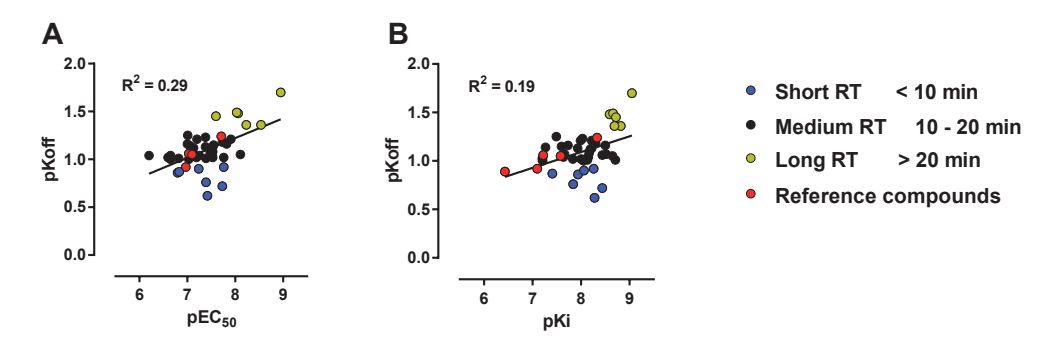


Figure S1. Correlation between potency (pEC₅₀) and dissociation rate (p k_{off}) (A); affinity (pK_i) and dissociation rate (p k_{off}) (B).

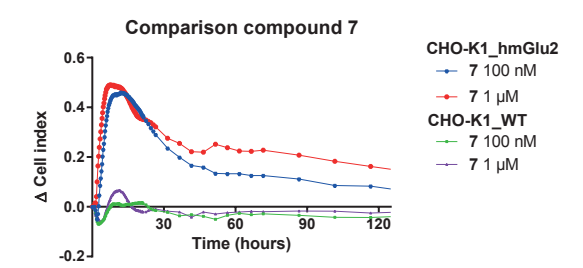


Figure S2. Comparison of PAM responses between CHO-K1 WT and CHO-K1_hmGlu $_2$ cells. Compound 7-induced responses: 100 nM (green) and 1 μ M (purple) on CHO-K1 WT cells (ATCC) and 100 nM (blue) and 1 μ M (red) on CHO-K1_hmGlu2 cells. 40,000 cells per well were added in a volume of 50 μ l. After resting for 30 minutes at room temperature, E-plates were placed in the recording station within a humidified 37°C, 5% CO2 incubator. Impedance was measured every 15 minutes overnight. After 18 hours, cells were stimulated with indicated concentration of compound. Impedance was measured every 15 seconds for 20 minutes, then 5 minute intervals were used for 40 minutes, followed by 15 minute intervals. A representative example is shown of a baseline-corrected response, which was repeated three times in duplicate.

Table S1. Selectivity data for representative mGlu₂ PAMs at mGlu_{13.4.5.6.7.8}.

hmGlu ₈ -anCa-pIC ₅₀	<4.6	<4.6	<4.6	
hmGlu ₈ -agCa-pEC ₅₀	<4.6	<4.6	<4.6	, ,
hmGlu ₇ -anCa-plC ₅₀	<4.6	<4.6	<4.6	<4.6
hmGlu ₇ -agCa-pEC ₅₀	<4.6	<4.6	<4.6	<4.6
rmGlu ₆ -anGT-pIC ₅₀	<4.52	<4.52	<4.52	<4.52
rmGlu ₆ -agGT-pEC ₅₀	<4.52	<4.52	<4.52	<4.52
hmGlu _s -anCa-plC ₅₀	<4.52	<4.52	V 5	<4.52
hmGlu _s -agCa-pEC ₅₀	<4.52	<4.52	<4.52	<4.52
hmGlu _s -pamCa_pEC ₅₀	<4.52	<4.52	<4.52	<4.52
hmGlu ₄ -anGT-plC ₅₀	<4.52	<4.52	<4.52	<4.52
hmGlu ₄ -agGT-pEC ₅₀	<4.52	<4.52	<4.52	<4.52
hmGlu ₃ -anCa-plC ₅₀	<4.52	<4.52	<4.52	<4.52
hmGlu ₃ -agCa-pEC ₅₀	<4.52	<4.52	<4.52	<4.52
hmGlu ₁ -anCa-plC ₅₀	<4.52	<4.52	<4.52	<4.52
hmGlu ₁ -agCa-pEC ₅₀	<4.52	<4.52	<4.52	<4.52
Compound	12	27	37	45

Ag, agonism; Ant, antagonism; PAM, positive allosteric modulation; Ca, data from calcium response in Ca²--based FDSS assay; GT, data from GTP S assay. All assays used human receptor except mGlu_e which used rat. Further details of methods can be found in Pérez-Benito et al. (2017).43